A UNITED STATES DEPARTMENT OF COMMERCE PUBLICATION

NBS MONOGRAPH 120

Unified Theory Calculations of Stark Broadened Hydrogen Lines Including Lower State Interactions

U.S. DEPARTMENT OF COMMERCE
National Bureau of Standards

UNITED STATES DEPARTMENT OF COMMERCE • Maurice H. Stans, *Secretary*

NATIONAL BUREAU OF STANDARDS • Lewis M. Branscomb, *Director*

Unified Theory Calculations of Stark Broadened Hydrogen Lines Including Lower State Interactions

C. R. Vidal, J. Cooper, and E. W. Smith

Radio Standards Physics Division
Institute for Basic Standards
National Bureau of Standards
Boulder, Colorado 80302

National Bureau of Standards Monograph 120

Nat. Bur. Stand. (U.S.), Monogr. 120, 45 pages (January 1971)
CODEN: NBSMA

Issued January 1971

Library of Congress Catalog Card Number: 79–608598

Table of Contents

Unified Theory Calculations of Stark Broadened Hydrogen Lines Including Lower State Interactions*

C. R. Vidal, J. Cooper, and E. W. Smith**

National Bureau of Standards, Boulder, Colorado 80302

Recently published calculations of hydrogen Stark broadening on the basis of the unified classical path theory have been extended to include lower state interactions in the final line profile. A detailed comparison with experiments in the density range 10^{13}–10^{17} cm^{-3} is given.

Key words: Classical path; hydrogen lines; line wings; Stark broadening; unified theory.

1. Introduction

In a recent paper [1],[1] henceforth referred to as paper I, the unified classical path theory [2] was generalized for the case of upper and lower state interactions and was applied to the Stark broadening of hydrogen. The thermal average of the time development operator and the final intensity profile of any hydrogen line were derived for the general case including lower state interactions. Numerical calculations for the thermal average including lower state interactions have been presented. The calculations of the final line profiles, however, have so far been restricted to the Lyman lines. In this paper we discuss calculations of the intensity profile including lower state interactions which are more involved because they require the evaluation of tetradic operators and contain more extensive sumations over vector coupling coefficients. The influence of lower state interactions is demonstrated for the first few lines of the Balmer series and possible simplifications for the higher series members are pointed out. A detailed comparison with various experiments covering the electron density range from about 10^{13}–10^{17} cm^{-3} is given requiring for low electron densities a convolution of the first series members with the Doppler profile. The unified theory calculations are also compared with static calculations. The applied computer program is presented in the appendix.

2. Basic Relations

In this section we summarize briefly the basic relations, which have been derived in paper I and are used for the unified theory calculations presented in this paper.

With the static ion field approximation the shape $I(\omega)$ of a Stark broadened line is given by

$$I(\omega)=\int_0^\infty P(\mathscr{E}_i)I(\omega,\mathscr{E}_i)d\mathscr{E}_i, \tag{1}$$

where the normalized distribution function $P(\mathscr{E}_i)$ is the low frequency component of the fluctuating electric microfields. In this manner we regard the radiator as being an atom subjected to a static field $\mathscr{E}_i$ and perturbed by the electrons. In the unified classical path theory [2] the ion field dependent line shape $I(\omega, \mathscr{E}_i)$ is obtained from

$$I(\omega,\mathscr{E}_i)=\frac{1}{\pi}\sum \mathrm{Im}\left\{\mathbf{d}\,\frac{1}{\Delta\omega_{\mathrm{op}}(\mathscr{E}_i)-\mathscr{L}[\Delta\omega_{\mathrm{op}}(\mathscr{E}_i)]}\,\mathbf{d}\right\}. \tag{2}$$

$\mathbf{d}$ is the dipole moment. The matrix elements of $\Delta\omega_{\mathrm{op}}$ specify the distance $\Delta\omega$ from a particular Stark component shifted by the static field $\mathscr{E}_i$ and $\mathscr{L}$ is essentially the Fourier transform of the thermal

*This research was supported in part by the Advanced Research Projects Agency of the Department of Defense, monitored by Army Research Office—Durham under Contract No. DA-31-124-AR0-D-139.

**Also at the Joint Institute for Laboratory Astrophysics and Department of Physics and Astrophysics, University of Colorado, Boulder, Colo. 80302.

[1] Figures in brackets refer to the literature references on p. 14.

average. Within the classical path approximation and the impact approximation $\mathscr{L}(\Delta\omega_{op})$ is given by

$$\mathscr{L}(\Delta\omega_{op}) = -i\Delta\omega_{op}\int_0^\infty \exp\ (+it\Delta\omega_{op})\overline{\mathscr{F}^{(1)}}(t)\,dt\Delta\omega_{op} \tag{3}$$

where the thermal average

$$\overline{\mathscr{F}^{(1)}}(t) = n_e \int d\mathbf{x}_1 d\mathbf{v}_1 \mathscr{W}(\mathbf{v}_1)[\mathscr{U}_1(\mathbf{R}, \mathbf{x}_1, \mathbf{v}_1, t) - 1]. \tag{4}$$

n_e denotes the electron density and $\mathscr{W}$ the velocity distribution function. The tetradic time development operator $\mathscr{U}_1$ is defined by the time ordered expression

$$\mathscr{U}_1(\mathbf{R}, \mathbf{x}_1, \mathbf{v}_1, t) = \mathscr{O} \exp\left\{-\frac{i}{\hbar}\int_0^t \tilde{\mathscr{V}}_1(\mathbf{R}, \mathbf{x}_1, \mathbf{v}_1, t')\,dt'\right\} \tag{5}$$

with the binary interaction

$$\tilde{\mathscr{V}}_1(\mathbf{R}, \mathbf{x}_1, \mathbf{v}_1, t) = \exp\{it\mathscr{H}_0/\hbar\}\mathscr{V}_1(\mathbf{R}, \mathbf{x}_1, \mathbf{v}_1, t) \exp\{-it\mathscr{H}_0/\hbar\}. \tag{6}$$

$\mathscr{V}_1$ is the Coulomb interaction potential between the radiator and a single perturbing electron. The Hamiltonian $\mathscr{H}_0$

$$\mathscr{H}_0 = \mathscr{H}_a + eZ\mathscr{E}_i \tag{7}$$

consists of the Hamiltonian $\mathscr{H}_a$ of the unperturbed radiator and the static ion part $eZ\mathscr{E}_i$. (For details see eqs (IV.16)–(IV.18),(III.14)–(III.16) and (II.2) of paper I.)

In evaluating the preceding equations for well isolated hydrogen lines we have to consider matrix elements only between states with the same principal quantum number n (no-quenching approximation) and it then is most convenient to work with parabolic states $|nqm\rangle$. m is the magnetic quantum number and the quantum number q is defined to be

$$q = n_1 - n_2 \tag{8}$$

with n_1 and n_2 being the usual parabolic quantum numbers which have to satisfy the relation

$$n = n_1 + n_2 + |m| + 1. \tag{9}$$

Furthermore, we distinguish quantum numbers which refer to the lower state from the upper state quantum numbers by a prime.

In taking matrix elements of the operators $\Delta\omega_{op}$, $\mathbf{d}$ and $\mathscr{L}(\Delta\omega_{op})$ between parabolic states it was shown in paper I that for the general case of upper and lower state interactions we have the following relations. For $\Delta\omega_{op}$, which is diagonal in parabolic states, one obtains

$$\langle n'q'm';\ nqm\,|\,\Delta\omega_{op}\,|\,n'q'm';\ nqm\rangle = \Delta\omega - \Delta\omega_i(n, q, n', q')\beta \tag{10}$$

where $\Delta\omega$ is the frequency perturbation from the position of the unperturbed line, β the normalized field strength in units of the Holtsmark field strength $\mathscr{E}_0$

$$\beta = \mathscr{E}_i/\mathscr{E}_0;\ \mathscr{E}_0 = \left(\frac{4\pi}{3}\right)^{2/3} e n_e^{2/3}. \tag{11}$$

and

$$\Delta\omega_i(n, q, n', q') = \left(\frac{4\pi}{3}\right)^{2/3}\frac{3}{2}(nq - n'q')\frac{\hbar}{m}\,n_e^{2/3}. \tag{12}$$

$\Delta\omega_i$ is the frequency shift of a particular Stark component characterized by the quantum numbers n, q, n' and q' due to the Holtsmark field strength $\mathscr{E}_0$. The matrix elements of $\mathscr{L}(\Delta\omega_{op})$ are given by

$$\langle n'q_b'm_b';\ nq_bm_b\,|\,\mathscr{L}(\Delta\omega_{op})\,|\,n'q_a'm_a';\ nq_am_a\rangle = -i\pi[\Delta\omega - \Delta\omega_i(n, q_b, n', q_b')\beta]^2$$
$$\sum_{q_cq_c'}\langle n'q_b'm_b';\ nq_bm_b\,|\,K(q_c, q_c')\,|\,n'q_a'm_a';\ nq_am_a\rangle i(\Delta\omega, \beta, n, n', q_b, q_b', q_c, q_c') \tag{13}$$

where

$$\langle n'q_b'm_b';\, nq_bm_b|K(q_c,q_c')|n'q_a'm_a';\, nq_am_a\rangle=(-1)^{m_a+m_b}\sum_{l_al_a'l_bl_b'Lm_cm_c'}(2L+1)$$
$$\langle n'q_a'm_a'|n'l_a'm_a'\rangle\langle n'l_a'm_c'|n'q_c'm_c'\rangle\langle n'q_c'm_c'|n'l_b'm_c'\rangle\langle n'l_b'm_b'|n'q_b'm_b'\rangle$$
$$\langle nq_am_a|nl_am_a\rangle\langle nl_am_c|nq_cm_c\rangle\langle nq_cm_c|nl_bm_c\rangle\langle nl_bm_b|nq_bm_b\rangle$$
$$\begin{pmatrix} l_a' & l_a & L\\ -m_c'm_cM'\end{pmatrix}\begin{pmatrix} l_a' & l_a & L\\ -m_a'm_aM\end{pmatrix}\begin{pmatrix} l_b' & l_b & L\\ -m_c'm_cM'\end{pmatrix}\begin{pmatrix} l_b' & l_b & L\\ -m_b'm_bM'\end{pmatrix}. \tag{14}$$

The unitary transformation $\langle nlm|nqm\rangle$ from parabolic to spherical states can be expressed in terms of $3j$-symbols [3]

$$\langle nlm|nqm\rangle=(-1)^{1/2(1+m-q-n)}\sqrt{2l+1}\begin{pmatrix}\frac{n-1}{2} & \frac{n-1}{2} & l\\ \frac{m-q}{2} & \frac{m+q}{2} & -m\end{pmatrix}. \tag{15}$$

Introducing the normalized time

$$s=\tilde{\omega}_pt \tag{16}$$

and the normalized frequency

$$\Delta\omega_R=[\Delta\omega-\Delta\omega_i(n,\,q_b,\,n',\,q_b')\beta]/\tilde{\omega}_p \tag{17}$$

with $\tilde{\omega}_p=\sqrt{8\pi n_ee^2/m}$ being the plasma frequency, the Fourier transform of the thermal average is defined to be

$$i(\Delta\omega_R,\,\beta,\,n,\,n',\,q_b,\,q_b',\,q_c,\,q_c')=\lim_{\epsilon\to0}\frac{1}{\pi}\int_0^\infty\exp\,[(-\epsilon+i\Delta\omega_R)s]\bar{F}(s,\,n,\,q_c,\,n',\,q_c')ds \tag{18}$$

The thermal average $\bar{F}(s)$ was evaluated in paper I for the general case of upper and lower state interactions and it was shown that $\bar{F}(s)$ may be approximated by a function $G(s)=\Sigma_kG_k(s)$ whose Fourier transform can be given analytically such that

$$i(\Delta\omega_R)=\sum_k i(k,\,\Delta\omega_R). \tag{19}$$

For most practical situations it turns out to be sufficient to consider only the first term in the series

$$i(k=1,\,\Delta\omega_R)=a_1b_1^2e^{-iZ_1}\left\{iH_0^{(1)}(Z_1)+H_1^{(1)}(Z_1)\left[1-\frac{i}{2Z_1}\right]\right\} \tag{20}$$

where $H_0^{(1)}$ and $H_1^{(1)}$ are Hankel functions and

$$Z_1=b_1\Delta\omega_R, \tag{21}$$

because the higher order terms usually affect the final line profile by not more than 2 percent around $\Delta\omega\simeq\tilde{\omega}_p$. The constants a_1 and b_1 are given by

$$a_1=-4\sqrt{\pi}\,n_eD^3C^2[B-\ln\,(4C^2)] \tag{22}$$

and

$$b_1=\frac{9}{4\pi^2}\,C[B-\ln\,(4C^2)]^2, \tag{23}$$

where D is the Debye length, B a constant of the order of unity (see table II in the appendix of paper I) and

$$C=\frac{3}{2}\,(nq-n'q')\,\frac{\hbar}{mDv_{av}}. \tag{24}$$

Finally we give for completeness the matrix elements of $d\otimes d$

$$\langle n'q_a'm_a';\ n'q_b'm_b' \mid d\otimes d \mid nq_am_a;\ nq_bm_b\rangle = (-1)m_a'\sum_{l_al_a'} \langle n'q_a'm_a' \mid n'l_a'm_a'\rangle\langle nl_am_a \mid nq_am_a\rangle$$

$$\begin{pmatrix} l_a' & l_a & 1 \\ m_a' & -m_a & \mu \end{pmatrix}\begin{pmatrix} l_a' & l_a & 1 \\ 0 & 0 & 0 \end{pmatrix}[(2l_a+1)(2l_a'+1)]^{1/2}\langle nl_a \mid r \mid n'l_a'\rangle$$

$$(-1)^{m_b'}\sum_{l_bl_b'} \langle n'q_b'm_b' \mid n'l_b'm_b'\rangle\langle nl_bm_b \mid nq_bm_b\rangle\begin{pmatrix} l_b' & l_b & 1 \\ m_b' & -m_b & \mu \end{pmatrix}\begin{pmatrix} l_b' & l_b & 1 \\ 0 & 0 & 0 \end{pmatrix}[(2l_b+1)(2l_b'+1)]^{1/2}\langle nl_b \mid r \mid n'l_b'\rangle \tag{25}$$

where the radial matrix elements are given in eq (63.2) of Bethe and Salpeter [4].

In case of no lower state interaction where the time development operator between lower states is replaced by a unit operator the matrix elements of $\mathscr{L}(\Delta\omega_{op})$ in eq (13) and (14) simplify significantly and we have

$$\langle n'q'm';\ nq_bm \mid \mathscr{L}_u(\Delta\omega_{op}) \mid n'q'm';\ nq_am\rangle = -i\pi[\Delta\omega-\Delta\omega_i(n,\ q_b,\ n',\ q')\beta]^2$$

$$\sum_{q_c}\langle nq_bm \mid K_u(q_c) \mid nq_am\rangle\, i(\Delta\omega,\ \beta,\ n,\ n',\ q_b,\ q',\ q_c) \tag{26}$$

where

$$\langle nq_bm \mid K_u(q_c) \mid nq_am\rangle = \sum_{l_a,\ m_c}\frac{1}{2l_a+1}\langle nq_am \mid nl_am\rangle\langle nq_bm \mid nl_am\rangle\,[\langle nl_am_c \mid nq_cm_c\rangle]^2. \tag{27}$$

Equation (26) simplifies even further for the Lyman lines with $|n'q'm'\rangle = |100\rangle$. For this case numerical calculations were given in paper I.

3. Properties of the $\mathscr{L}$ and K Matrix

In eqs (13) and (26) we have split the $\mathscr{L}$-matrix into two parts. One part, the K-matrix, contains all the vector coupling coefficients or $3j$-symbols and is independent of the plasma parameters, while the other part, the Fourier transform of the thermal average $i(\Delta\omega)$, contains all the broadening parameters. The K-matrix is completely specified by the upper and lower state principal quantum numbers n and n' and needs to be calculated only once for every hydrogen line.

From eq (14) we realize first of all that the K-matrix is symmetric to the diagonal

$$\langle n'q_b'm_b';\ nq_bm_b \mid K(q_c, q_c') \mid n'q_a'm_a';\ nq_am_a\rangle = \langle n'q_a'm_a';\ nq_am_a \mid K(q_c, q_c') \mid n'q_b'm_b';\ nq_bm_b\rangle \tag{28}$$

while the $\mathscr{L}$-matrix is not, due to the factor $[\Delta\omega-\Delta\omega_i(n,\ q_b,\ n',\ q_b')\beta]^2$. Next we see from the $3j$-symbols that K is diagonal in the quantum number M.

$$M = m_a'-m_a = m_b'-m_b \tag{29}$$

Hence we may arrange the K-matrix and also the $\mathscr{L}$-matrix in such a manner that they are block diagonal in M, where $M=0, \pm1, \pm2, \ldots, n+n'-2$. We also notice that matrix elements which differ only in the sign of M are identical.

$$\langle n'q_b'-m_b';\ nq_b-m_b \mid K(q_c,\ q_c') \mid n'q_a'-m_a';\ nq_a-m_a\rangle$$

$$= \langle n'q_b'm_b';\ nq_bm_b \mid K(q_c,\ q_c') \mid n'q_a'm_a';\ nq_am_a\rangle \tag{30}$$

Consequently, blocks which differ in the sign of M, can also be made identical. This greatly simplifies the matrix inversion required by eq (2). The problem is further simplified by the fact that also the $d\otimes d$-matrix can be made block diagonal in

$$\mu = m_a - m_a' = m_b - m_b', \tag{31}$$

where μ can only take on the values 0 and ± 1. As a result we finally have to evaluate only the blocks with $M=0$ and $M=1$ of the K and $\mathscr{L}$-matrix, respectively, because the block with $M=-1$ gives identically the same contribution to the final line profile as the block with $M=1$ and all the other blocks with $|M|>1$ do not contribute due to the $d\otimes d$ matrix. Further useful symmetry properties of the K-matrix are given in the following equations:

$$\begin{aligned}\langle n' q_b' m_b' ;\, n q_b m_b |\, K(q_c, q_c') \mid n' q_a' m_a';\, n q_a m_a\rangle \\ = \langle n' - q_b' - m_b';\, n - q_b - m_b \mid K(q_c, q_c') \mid n' - q_a' - m_a';\, n - q_a - m_a\rangle \\ = \langle n' q_b' m_b';\, n q_b m_b \mid K(-q_c, -q_c') \mid n' q_a' m_a';\, n q_a m_a\rangle .\end{aligned} \tag{32}$$

The latter relation simplifies our summation over q_c and q_c' in eq (13) because also for the Fourier transform $i(\Delta\omega)$ we have

$$i(\Delta\omega, \beta, n, n', q_b, q_b', q_c, q_c') = i(\Delta\omega, \beta, n, n', q_b, q_b', -q_c, -q_c') \tag{33}$$

In calculating $I(\omega, \mathscr{E}_i)$ according to eq (2) we always have to invert complex matrices. Since for computational purposes it is more convenient to work with real matrices and since we need only the imaginary part of the inverted matrix we make use of the following relations

$$X + iY = [A + iB]^{-1}$$

where

$$X = [A + BA^{-1}B]^{-1} \tag{34}$$

$$Y = -[B + AB^{-1}A]^{-1}$$

with X, Y, A and B being real matrices. From eqs (2), (13) and (18) it is clear that A contains the diagonal matrix of $\Delta\omega_{op}$ and the sine transform of the thermal average and B the cosine transform of the thermal average. In the limit of large $\Delta\omega$ we have

$$A = B + \Delta\omega \cdot I \tag{35}$$

(see eq (X.18) of paper I) which simplifies to lowest order the Y-matrix to

$$Y \simeq -B/\Delta\omega^2 \tag{36}$$

This is the one electron limit, which as pointed out already in section IV. of paper I, does not require a matrix inversion.

4. The Influence of Lower State Interactions and the Static Limit

In the figures 1, 2, 3, 7 and 8 the intensity of the line is plotted versus the frequency perturbation $\Delta\omega$ in units of the plasma frequency $\tilde{\omega}_p = \sqrt{8\pi n e^2/m}$. The frequency scale is preferred, because it represents essentially the energy perturbation and is therefore more meaningful for the discussion of Stark broadening than, for example, the wavelength scale, which is usually more convenient in the measurement. Furthermore, $\Delta\omega/\tilde{\omega}_p \lesssim 1$ is essentially the domain of the unmodified impact theory.

We first demonstrate the influence of lower state interaction on the final line profile in figures 1 and 2 and compare three different methods of evaluation. In the first, most general method lower state interactions are taken into account and the line profiles are calculated on the basis of eqs (13) and (14) using the correct Stark effect for electrons and ions (solid curves in fig. 1). In the second method based on eqs (26) and (27) we neglect lower state interactions for the electrons, i.e., we do

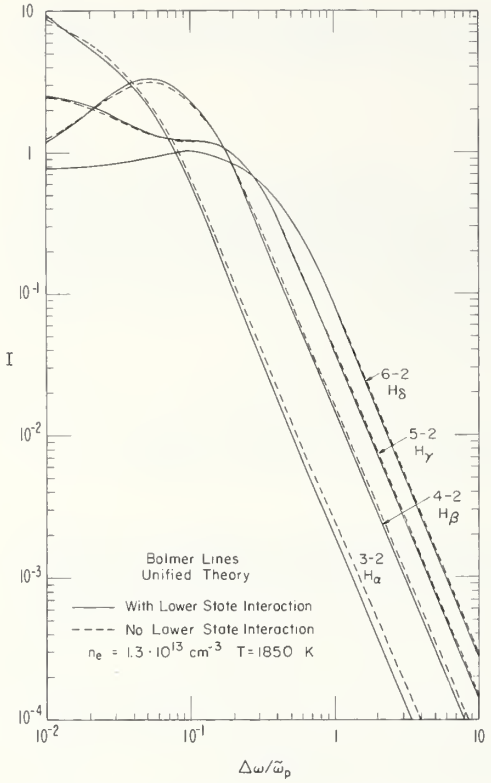

FIGURE 1. *The influence of lower state interactions on the Balmer lines H_α to H_δ.*

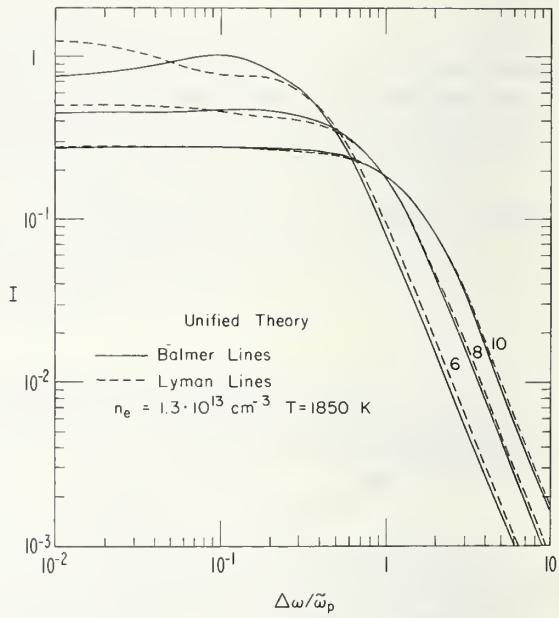

FIGURE 2. *Comparison of the Balmer and Lyman lines with the upper state principal quantum numbers* n=6, 8 *and* 10.

not allow for perturbations of the lower state sublevels by electrons (dashed curves in fig. 1, solid curves in fig. 2). However, we still use the correct Stark effect for the static ions. In the third and simplest method the line profiles are calculated like in case of the Lyman lines with no influence of the lower state for the electrons as well as the static ions (dashed curves in fig. 2). These Lyman profiles have been presented previously in Paper I.

We realize first of all from figure 1 that in view of the accuracy to be expected from the unified classical path theory we may neglect lower state interaction due to the electrons for H_δ and therefore also for all the higher Balmer lines. For $n_e = 1.3 \cdot 10^{13}$ cm^{-3} and $T = 1850$ K the biggest calculated difference between the cases with and without lower state interaction is 43 percent for H_α, 10 percent for H_β, 6 percent for H_γ and 4 percent for H_δ. These differences have been obtained for the distant, almost quasistatic wing. They become slightly smaller in the purely static wing and are significantly smaller in the line center (14% for H_α, 9% for H_β, and 3% for H_γ and 2% for H_δ). Similar differences may be obtained at any electron density and temperature. In the distant, purely static wing the difference will always be identical (39.2% for H_α, 9.3% for H_β, 5.7% for H_γ and 3.6% for H_δ), because the static ions are treated in both cases with the same, correct Stark effect, while the static electrons are treated in the second method with the Stark effect of the corresponding Lyman line.

In figure 2 the Balmer lines and the Lyman lines with the upper state principal quantum numbers $n = 6, 8$ and 10 are compared. In the line center we recognize the fact that the even Balmer lines have no unshifted Stark component, while the even Lyman lines do. The difference in the wings is also clear from the Stark effect of the Balmer and Lyman lines (see also table I of the paper by Vidal [5]). It therefore becomes apparent that for principal quantum numbers of about $n > 10$ one may neglect the influence of the lower states on the final line profile altogether and use the Lyman profiles throughout.

Next we compare in figure 3 the results of the unified classical path theory (solid curves) with quasistatic calculations (dashed curves) in order to show to what extent quasistatic calculations may be useful. The even Balmer lines up to $n = 14$ are plotted. The quasistatic profiles are based

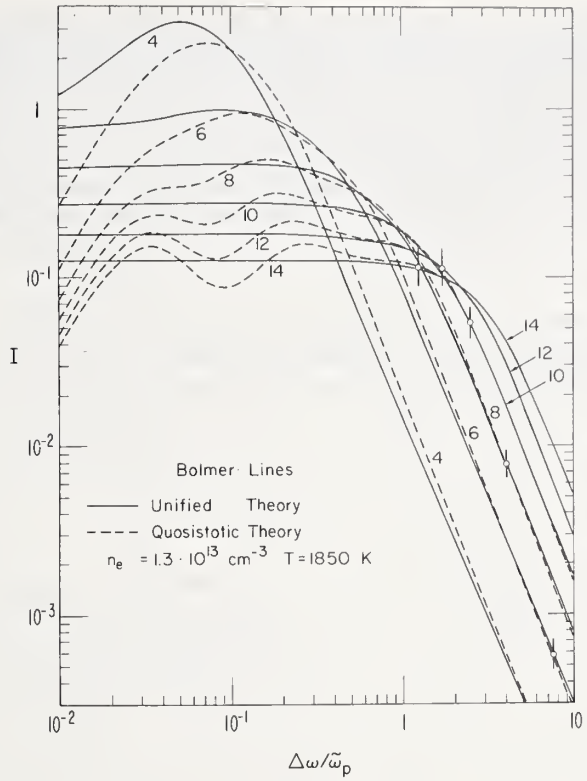

FIGURE 3. *Comparison of the unified theory and the quasistatic theory for the even Balmer lines with* n=4 *to* n=14.

on the low frequency component of the electric microfield distribution functions [6, 7] with a shielding parameter

$$r_0/D = 0.0898 n_e^{1/6}/\sqrt{T} \tag{37}$$

and the total density N being $N=2n_e$. In addition, short vertical lines mark the position of the average Weisskopf frequency

$$\Delta\omega_c = 2mv_{av}^2/(3\pi^2\bar{n}_k\hbar) \tag{38}$$

as defined by Unsöld [8], where the average splitting

$$\bar{n}_k = \sum_k n_k f_k / \sum_k f_k \tag{39}$$

with f_k being the oscillator strength of the kth Stark component is frequently approximated by $\bar{n}_k \simeq n(n-1)/2$ (see table I of the paper by Edmonds, Schlüter and Wells [9]). The Weisskopf frequency indicates the domain of the quasistatic theory and there have been various estimates, which all agree within a factor of 2 to 3. From figure 3 it is apparent that with increasing principal quantum numbers the profiles based on the unified classical path theory approach more and more the static profiles and that the Weisskopf frequency turns out to be a rather conservative estimate for the useful range of the quasistatic theory. In the example presented we recognize that except for the very line center one may use quasistatic calculations almost throughout the entire profile for principal quantum numbers of $n \gtrsim 10$. For practical purposes the hole in the center of the static profile and the structure in the line center, which for the higher series members appears to oscillate around the profile based on the unified classical path theory, will be smeared out by a convolution with the Doppler profile.

5. Comparison With Experiments and Other Theories

We start our comparison of the unified theory with experiments in the high and low electron density range with recent measurements by Wiese, Kelleher, and Paquette [10] performed on a

high current, wall-stabilized arc. The experimental setup and the method of evaluation is similar to the one described by Wiese, Paquette, and Solarski [11]. However, a number of refinements are incorporated in the experimental setup and the achievable accuracy has been greatly improved.

In figure 4 and 5 the red and blue wings of the measured H_β- and H_γ-profiles are plotted (solid lines), which have been obtained in the same run assuring the same electron density and temperature for both profiles. For the moment we do not consider the asymmetries of the profile, since the theory is not yet arranged to describe them. The electron density and temperature for this particular run have been determined in several ways from the absolute intensity of H_β with

$$n_e = 7.5 \cdot 10^{16}\ \text{cm}^{-3} \qquad T = 12570\ \text{K},$$

from the absolute intensity of H_γ with

$$n_e = 7.7 \cdot 10^{16}\ \text{cm}^{-3} \qquad T = 12640\ \text{K}$$

and from the absolute intensity of the continuum in the visible and in the UV, which differ by the contribution from the Balmer continuum, with

$$n_e = 8.0 \cdot 10^{16}\ \text{cm}^{-3} \qquad T = 12730\ \text{K}.$$

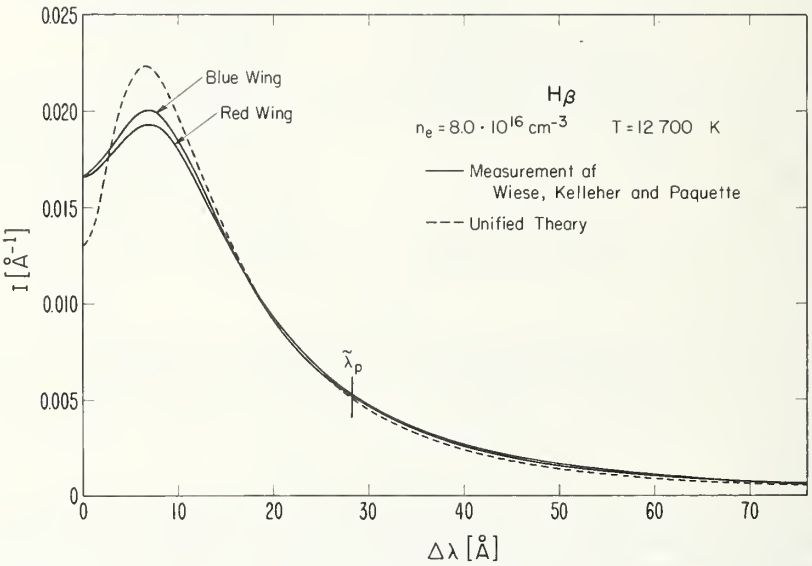

FIGURE 4. *Comparison between the unified theory for H_β and the experimental profile as measured by Wiese, Kelleher and Paquette.*

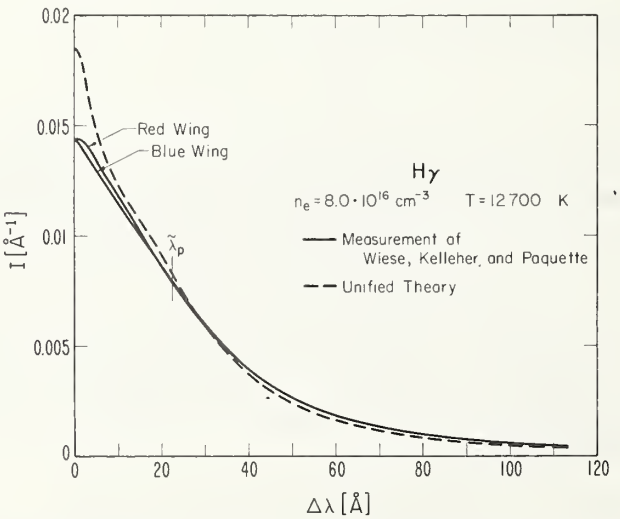

FIGURE 5. *Comparison between the unified theory for H_γ and the experimental profile as measured by Wiese, Kelleher and Paquette.*

The three values of the electron density differ in all runs by similar amounts. In particular the difference between the values from the H_β and the continuum intensity is very reproducible and gives rise to a 6 percent difference in the electron density. There are indications (private communication of Dr. Wiese) that these differences may be due to small non LTE (local thermodynamic equilibrium) effects in the arc because of its rather small dimension. This would be consistent with the validity criteria for LTE in inhomogeneous stationary plasmas (see section 6–10 of Griem [12]). Since the continuum intensity is least affected, the electron density and temperature as obtained from the continuum have been adopted as the best values, in particular, since the same values have been obtained from the continuum in the visible and the UV. For these parameter values the profiles as calculated with the unified theory including lower state interactions have been plotted in figures 4 and 5 with the same normalization $\int_{-\infty}^{+\infty} I(\Delta\lambda)d\lambda = 1$ as the experimental profiles. We realize that the calculated profiles are slightly higher and narrower than the measured profiles. In *both* cases, however, the best agreement between theory and experiment in a least squares sense has been obtained with $8.5 \cdot 10^{16}$ cm^{-3}, meaning that the theoretical value appears to be 6 percent larger than the experimental value.

Applying recent calculations of Kepple and Griem [13], one obtains from the half-, quarter-, and eighth-width $n_e = 7.38 \cdot 10^{16}$ cm^{-3} for H_β and $n_e = 8.05 \cdot 10^{16}$ cm^{-3} for H_γ (as evaluated by Dr. Wiese), which reveals an intrinsic inconsistency because the two electron densities differ by about 10 percent.

We also notice that the worst agreement is in the very line center, a feature which is so far common to all impact theories. This fact makes the determination of the electron density on the basis of fractional widths rather questionable because its definition may be ambiguous and it effectively normalizes wing intensities with respect to the intensity in the very line center, where the theory seems to be least reliable. Although this is the most convenient and most widely used method, it is definitely preferable to determine the electron density from a least squares fit of the experimental and theoretical profile using the same normalization for both profiles.

In figure 6 the calculations of Kepple and Griem [13] are compared with our calculations for H_β and $n_e = 6.4 \cdot 10^{16}$ cm^{-3} and $T = 12.200$ K indicating that our profile is narrower and higher,

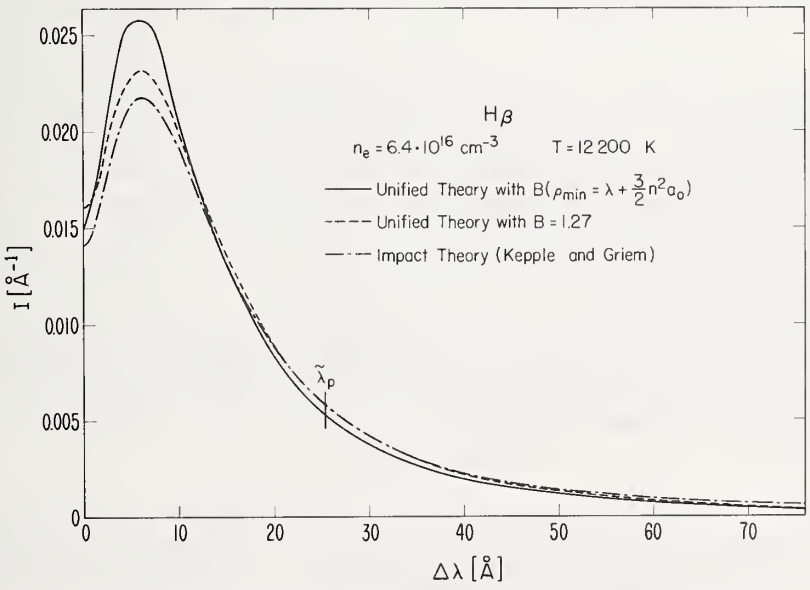

FIGURE 6. *Comparison between the unified theory with B as obtained for* $\rho_{min} = \lambda + \frac{3}{2}n^2a_0$, *with* $B = 1.27$ *as used by Kepple and Griem and the modified impact theory of Kepple and Griem.*

hence giving rise to larger electron densities. In the very line center the most important difference appears to be due to the constant B in eqs (22) and (23). While our calculations are based on a quantum number dependent constant B for a lower cutoff $\rho_{\min} = \lambda + \frac{3}{2} n^2 a_0$, which has been selected according to the validity criterion of the classical path theory, Kepple and Griem use a

larger value $B = 1.27$ for all the Stark components. We have repeated our calculations with their value of the constant B. The profile is included in figure 6 and does not quite agree with their calculations. It should be pointed out that the normalization of the profile of Kepple and Griem is slightly too small, which may account for part of the remaining difference in the very line center, where the unified classical path calculations should go over to the results of the impact theory, if the ion field dependent cutoff (see eq. VI.4 of paper I) is neglected.

From the preceding comparison we realize that at this stage the most important problem seems to be to obtain better values of the constant B whose dependence on various cutoff procedures was discussed in the appendix of paper I for classical path theories neglecting time ordering. We note that in case of the H_β and H_γ profiles in figures 4 and 5, better agreement between theory and experiment may be obtained with a constant B larger than that used in this paper, and that in case of the Lyman-α experiment of Boldt and W. S. Cooper [14] discussed in paper I, better agreement is obtained with a smaller constant B.

For the moment we postpone the discussion of the various possibilities, which may affect the constant B, until we also have compared our results with measurements of the Balmer lines H_3–H_{14} and the Paschen lines P_6–P_{13} performed by Vidal [5, 15]. Unfortunately, these experiments do not provide an independent electron density measurement, which is as accurate as the measured profiles. Since, however, the measurements revealed a $\Delta\omega^{-5/2}$-wing, which for most of the lines extended over two orders of magnitude in intensity, the electron density was determined assuming that these measured $\Delta\omega^{-5/2}$-wings were identical to the asymptotic Holtsmark wings. In this manner the same electron density of $n_e = 1.3 \cdot 10^{13}$ cm^{-3} was obtained within ± 4 percent for all the Balmer lines from H_4–H_{14} (see Vidal [5]). In paper I it was pointed out (on the basis of the Lyman line calculations) that the unified theory calculations actually give the $\Delta\omega^{-5/2}$-wings which were measured in the experiment and which extend much further into the line center than a quasistatic theory would predict. However, over the intensity range measured, these $\Delta\omega^{-5/2}$-wings do not necessarily coincide with the asymptotic Holtsmark wing.

In the following we reevaluate the measured line profiles employing now the complete line profile from the line center to the wings. We concentrate primarily on the Balmer lines, which have been measured more accurately than the Paschen lines and where we also have more series members available. The measurements were performed on a stationary radio frequency discharge within a magnetic bottle as described by Schlüter [16]. The electron temperature, which within the error limits is equal to the ion temperature, was measured to be $T = 1850$ K. Consequently, we have to consider first of all to what extent Doppler broadening and the Zeeman effect may influence the first series members. In figure 7 the theoretical line profiles are shown for $n_e = 1.3 \cdot 10^{13}$ cm^{-3} and $T = 1850$ K before (dashed lines) and after (solid lines) the convolution with the Doppler profile. It shows that up to around H_8 Doppler broadening has to be taken into account. In estimating the influence of the Zeeman effect we notice that for a magnetic field of 1800 gauss (0.18 tesla) as typically used in the experiments, the separation of the outer components of the Lorentz triplet amounts to 0.168 cm^{-1}. Neglecting complications due to the combined Zeeman and Stark effect this indicates that from around H_7 (full half width $= 1.76$ cm^{-1}) we may neglect the Zeeman effect for all the higher series members.

A comparison of the experimental and theoretical profiles for the Balmer lines H_7–H_{14} gives the best agreement for $n_e = 1.15 \cdot 10^{13}$ cm^{-3}, a value which is slightly smaller than the value of $n_e = 1.3 \cdot 10^{13}$ cm^{-3} given by Vidal [5]. This is not surprising because within the measured intensity range the apparent $\Delta\omega^{-5/2}$-wings of the unified theory calculations are all lying above the asymptotic Holtsmark wings on which the electron density value of Vidal [5] was based. For this new value the measured and calculated Balmer lines H_7–H_{14} all agree within 5 percent over the entire line profile. These maximum deviations are comparable to the achieved accuracies of the measurement and are so small that they hardly show up in a plot like in the figures 1, 2, 3, 7, and 8. For the lower Balmer lines only the line wings can be evaluated since the line center is noticeably affected by the Zeeman effect not included in the calculations. The agreement is not quite as good. However, the differences do not exceed 10 percent for the wings of H_β to H_δ, which appears to be partially due to the growing influence of the apparatus profile for the narrower profiles of the lower series members.

In figure 8 our calculations are compared with the calculations of Kepple and Griem [13], which have been extended to H_{12} by Bengtson, Kepple and Tannich [17]. We see that their profiles are wider and that the higher series members do not show the measured $\Delta\omega^{-5/2}$-wings. From a comparison with figure 3 we also realize that with increasing principal quantum number n our profiles approach the static profiles while the profiles of Kepple and Griem do not. Their profiles actually appear to differ more and more from the static profiles with increasing principal quantum number n, which manifests the fact that the modified impact theory is not able to describe the static electrons.

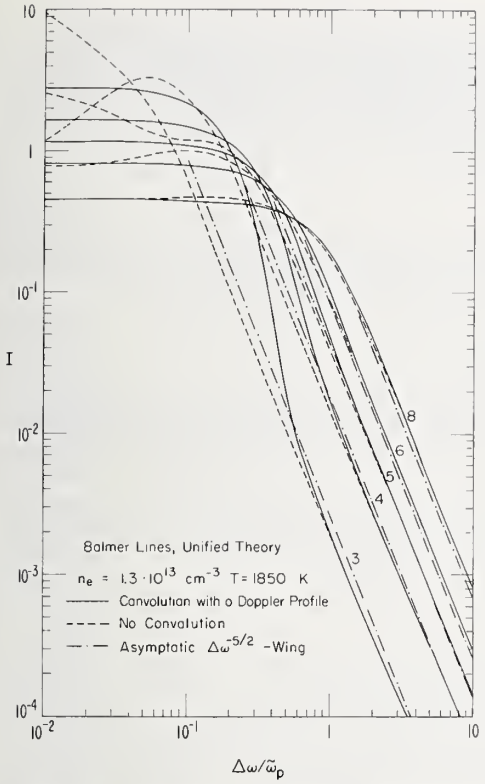

FIGURE 7. *The Balmer line profiles as calculated with the unified theory for* $n_e = 1.3 \cdot 10^{13}\ cm^{-3}$ *and* $T = 1850\ K$ *with and without the convolution of the Doppler profile.*

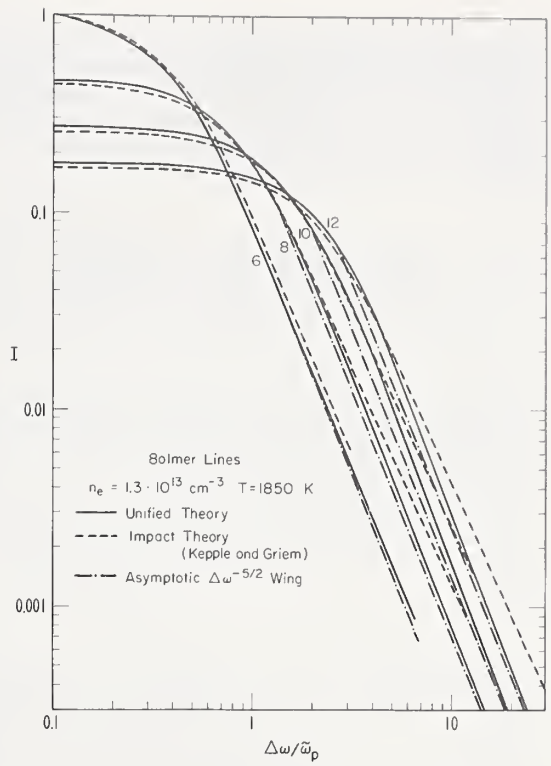

FIGURE 8. *Comparison between the unified theory and the modified impact theory of Kepple and Griem for the even Balmer lines* H_6 *to* H_{12}.

As pointed out already in paper I, we emphasize again that contrary to the H_β- and H_γ-profiles discussed above, the higher series members are insensitive to the exact value of the constant B. The reason is that these profiles are predominantly static in nature. In other words it means that the average Stark effect splitting, which is approximately equal to the half width of the higher series members, is significantly larger than the constants a_1 for the different Stark components (see eq (22)), which determine essentially the electron impact broadening. Since the line centers of the first series members are predominantly Doppler broadened, these low density experiments give no detailed information on the constant B. Hence, as one would expect, we also obtain a better agreement between theory and experiment than we did for the H_β- and H_γ-profiles discussed above, where the agreement could have been worse due to the uncertainty of the constant B. This fact is particularly important for astrophysical applications where one is mainly interested in low density profiles, because these profiles are insignificantly affected by the remaining uncertainty of the constant B. One may, therefore, calculate low density profiles with rather large confidence.

6. Discussion

Since the value of the constant B appears to be the most vague and restricting quantity in the current classical path theories, we will now summarize the effects which may influence the constant B and are not included in the present calculations. First of all, we can state in general that the exact value of the constant B is least important if either the static broadening exceeds the electron impact broadening, as discussed above for the low density profiles, or if according to eq (22) the value of $\ln(4C^2)$ is much larger than the uncertainty of the constant B which means that

$$-\ln(4C^2) \gg 1. \tag{40}$$

According to eq (24) the latter situation is most likely to occur for the innermost Stark components of any hydrogen line.

The constant B is sometimes misleadingly referred to as the strong collision parameter. This is only partially correct, because its value depends not only on the lower cut off parameter ρ_{min}

but also on the upper cut off parameter αD, where D is the Debye length and the constant α has been varied in the literature from 1.1 (Griem, Kolb and Shen [18]) down to 0.6 (Chappell, J. Cooper and E. Smith [19]). As discussed in the appendix of paper I, this parameter α will also influence the limits on the time integral $\int V(t')dt'$ in the time development operator $\mathcal{U}$, which for the S-matrix limit are extended from $-\infty$ to $+\infty$. In the unified theory calculations these limits have been extended from $-T$ to $+T$, where

$$T = \sqrt{\alpha^2 D^2 - \rho^2}/v, \tag{41}$$

in order to make the time limits consistent with the upper cut off parameter αD. We also saw from the appendix of paper I that, as a function of the parameter α, the constant B varies as

$$B = B(\alpha = 1) + 2 \ln \alpha. \tag{42}$$

The correct value of the constant α has not yet been determined conclusively. Since for large impact parameters one is dealing only with weak collisions, it has to be possible to determine the parameter α from a second order classical path theory, which means essentially within the frame work of the ordinary impact theory.

The influence of small impact parameter collisions on the constant B is a much more involved problem. First of all, it is clear that one has to worry about collisions with impact parameters

$$\rho \gtrsim \rho_{\min} = \lambda\!\!\!^{-} + \tfrac{3}{2}\, n^2 a_0 = \lambda\!\!\!^{-}\,(1 + 3.78 \cdot 10^{-3}\, n^2 \sqrt{T}\,) \tag{43}$$

where classical path theories start to break down. As discussed for example, by E. W. Smith, C. R. Vidal and J. Cooper [20] we have to distinguish in this range between "completed" strong collisions, which contribute primarily to the impact limit, and "incompleted" strong collisions, which mostly contribute to the static wings. While the latter collisions are properly treated in a classical path theory and have no influence on the value of the constant B, the "completed" strong collisions can only be treated correctly by a quantum mechanical calculation, which has not yet been done.

Besides the limitation imposed by a classical path approach, we also have to consider the influence of time ordering which has been neglected in our time development operator $\mathcal{U}$ of eq (5). We notice that time ordering will become important if $V\tau/\hbar \gtrsim 1$. With a typical collision time $\tau \simeq \rho/v$, this is the case for impact parameters

$$\rho \gtrsim \rho_{\text{ord}} = \tfrac{3}{2}\,(nq - n'q')\,\lambda\!\!\!^{-}. \tag{44}$$

For most practical cases, where the value of B becomes critical, ρ_{ord} is larger than $\rho_{\min}$. Hence, there will be a domain, in which time ordering is important even within the region of validity of a classical path theory.

In the S-matrix limit the effect of time ordering has been investigated within the classical path theory for Ly_α (Bacon, Shen, and J. Cooper [21]) and for H_α (Bacon [22]) by solving the complete set of coupled differential equations, which define all the matrix elements of the time development operator. These calculations have demonstrated that the effect of time ordering may change the value of the constant B by as much as ± 1 and that the effect on the final line profile may amount to a few percent in intensity. These calculations have also included higher multipole terms. If one examines the effect of the higher multipole terms with respect to the case, where one considers only the dipole terms, one finds out that in case of Lyman-α as well as in case of H_α the higher multipole terms lower the value of all the different constants B. However, at the electron density and temperature of these experiments (which are essentially the same), the change in the constant B due to the higher order multipole terms affects the final line profile only very little.

For the more general case of the time development operator $\mathcal{U}$, required by the unified theory, the effect of time ordering has recently been examined for Lyman-α [23]. These calculations show the results of the S-matrix limit in the line center and the decreasing influence of time ordering with increasing frequency pertubation $\Delta\omega$.

Due to the various outlined reasons which may affect the value of the constant B, it is rather difficult to make a quantitative statement of the possible error. If we assume that for impact parameters $\rho \gtrsim \rho_{\text{ord}}$ all the collisions which contribute to the value of B, have been treated correctly, one may give an upper bound on the possible error in B based on the unitarity condition of the time

development operator. Since the time development operator may only oscillate within the limits of ± 1, the integral over impact parameters from 0 to ρ_{ord}, which is weighted by the impact parameter ρ, will change the constant B at the most by an amount of the order of unity. In addition to this the influence of the upper cut off parameter according to eq (42) has to be kept in mind. We also recall that in order to obtain the best agreement between theory and experiment we have to change the constant B for the Lyman α profile [14] by an amount which is slightly larger than 1, and for the H_β and H_γ profile by an amount, which is smaller than 1. It should also be noted that the ion field splitting is not fully taken into account in the time development operator as discussed in section VI of paper I. It was shown that this may lead to slight modifications in the line center but not in the line wings. A full treatment would be rather difficult because the ion field exponentials in eq (VI. 4) of paper I remove the spherical symmetry of the problem and a simple cut off procedure as suggested by Kepple and Griem [13] does not appear to be completely adequate since it affects the normalization of the line profile. In addition, near the line center we would expect the quasistatic description for the ions to be invalid. This however, is practically unimportant because the Weisskopf frequency for the ions, which gives the range of validity for a quasistatic approach, is for low densities well inside the Doppler width and at high densities well inside the half width. Notice also that the breakdown of the no-quenching approximation may cause a small effect on the strong collision term (see ref. [20], p. 415).

So far we have ignored profile asymmetries which have been observed, for example, in Ly-α, H_β and H_γ. In the following we give a brief discussion in which we do not consider the well known asymmetries due to the ω^4-factor in the expression for the power spectrum, the frequency to wavelength conversion, and the Boltzmann factor [24], which was neglected by assuming the elements of the atomic density matrix to be constant for all initial states. Asymmetries due to these effects will grow with increasing frequency perturbation $\Delta\omega$ and are always negligible in the line center. Hence, we are mainly concerned with the higher order multipole terms and the higher order Stark effect terms due to the electrons and ions.

In section VII of paper I it was shown how the higher order multipole terms due to the electron perturbers can be included in the interaction potential of the time development operator and it was pointed out that within the no-quenching assumption only a finite number of multipole terms exist. The main aggravation is that the unitary transformation which diagonalizes the time development operator after the spherical average is no longer a simple rotation. In the impact limit this will affect primarily the constant B as noted above and cause only negligible asymmetries like in case of the time ordered solutions [21, 22].

The main reason for asymmetries especially in the line center has been shown to be due to the ions and we refer to a recent paper of Sholin [25] which supersedes the earlier papers by Griem [26] and Nguyen-Hoe, Drawin and Herman [27]. In this paper, it has been successfully demonstrated that the observed asymmetries of the Ly-α, H_β and $H\gamma$-lines can all be explained within a static ion approach, where the main effect is caused by the quadrupole term of the ions and to a smaller extent by the quadratic Stark effect and the ion field dependent transition probability corrections of the individual Stark components. The electrons were assumed to cause only collision broadening and to introduce no further asymmetries.

It should be pointed out that the results presented by Sholin can easily be incorporated into the calculations presented here and work on this is in process. Like Sholin, we regard the radiator as being an atom in a static ion field $\mathscr{E}_i$ and perturbed by the electrons. Hence, one only has to modify the matrix elements of $\Delta\omega_{op}$ in eq (10) and of $d\otimes d$ in eq (25) according to the relations given by Sholin, in order to include the higher order multipole terms and the higher order Stark effect terms due to the static ions.

If we incorporate the higher multipole terms due to the electrons in the time development operator together with those due to the ions, another interesting feature of the unified theory is that a number of the higher order multipole terms due to the electrons and ions like, for example, the most important quadrupole terms, will cancel each other in the static limit of the electrons. This effect was already suspected by Griem [12] (p. 94). However, this sort of mutual compensation occurs only if electrons and ions are treated within the framework of the same approximations (for example, quasi-static or impact) as pointed out by Sholin [25]. For this reason the occurrence of asymmetries gives important information on the type of electron broadening. It is also clear why asymmetries have been observed in the high density profiles of Ly_α, H_β and $H\gamma$, where the ions may be treated quasi-statically and the electrons are over most of the measured line profile in the domain of the impact theory, but not in the low density profiles of the higher Balmer and Paschen lines, where ions and electrons are both in the quasi-static domain over almost the entire line profile.

Finally, we may conclude that, at this stage, the accuracy of the unified theory calculations depends primarily on the extent to which the final line profile is affected by the constant B and

406-848 O - 71 - 2

to a lesser extent on the asymmetries not yet included. Both effects are in turn determined by the electron density and temperature. It is probably safe to say that in general the electron density obtained with the unified theory in its present form will differ at the most by 10 percent from its true value. In the impact limit significantly better agreements between theory and experiment, which have been reported in the literature, have to be regarded as fortuitous. However, better results are definitely obtained for the higher, still well isolated series members and/or at low electron densities ($n_e \lesssim 10^{13}$ cm^{-3}), which are of particular astrophysical interest.

7. References

[1] Vidal, C. R., Cooper, J., and Smith, E. W., J. Quant. Spectr. Radiative Transfer, **10**, 1011 (1970).
[2] Smith, E. W., Cooper, J., and Vidal, C. R., Phys. Rev. **185**, 140 (1969).
[3] Hughes, J. W. B., Proc. Phil. Soc. **91**, 810 (1967).
[4] Bethe, H. A., and Salpeter, E. E., Quantum Merchanics of One- and Two-Electron Atoms (Springer Verlag, Berlin 1957).
[5] Vidal, C. R., Proc. of the 7th Intern. Conf. on Phenomena in Ionized Gases, p. 168 (1966).
[6] Baranger, M., and Mozer, B., Phys. Rev. **115**, 521 (1959); **118**, 626 (1960).
[7] Hooper, C. F., Phys. Rev. **165**, 215 (1968).
[8] Unsöld, A., Physik der Sternatmosphären (Springer Verlag, Berlin 1955).
[9] Edmonds, F. N., Schlüter, M., and Wells, D. C., Mem. Roy. Astr. Soc. **71**, 271 (1967).
[10] Wiese, W. L., Kelleher, D. E., and Paquette, D. R., to be published. (The authors would like to thank Dr. Wiese for making his measurements accessible to us prior to publication).
[11] Wiese, W. L., Paquette, D. R., and Solarski, J. E., Phys. Rev. **129**, 1225 (1963).
[12] Griem, H. R., Plasma Spectroscopy (McGraw-Hill Book Co., Inc., New York, 1964).
[13] Kepple, P., and Griem, H. R., Phys. Rev. **173**, 317 (1968). see also University of Maryland, Report 831.
[14] Boldt, G., and Cooper, W. S., Z. Naturforschung **19a**, 968 (1964).
[15] Vidal, C. R., Z. Naturforschung **19a**, 947 (1964).
[16] Schlüter, H., Z. Naturforschung **15a**, 281 (1960).
[17] Bengtson, R. D., Kepple, P., and Tannich, J. D., Phys. Rev. **A1**, 532 (1970).
[18] Griem, H. R., Kolb, A. C., and Shen, K. Y., Astrophys. J. **135**, 272 (1962).
[19] Chappell, W. R., Cooper, J., and Smith, E. W., J. Quant. Spectr. Radiative Transfer **9**, 149 (1969).
[20] Smith, E. W., Vidal, C. R., and Cooper, J., J. Res. Nat. Bur. Stand. (U.S.), **73A** (Phys. and Chem.), No. 4, 405 (1969).
[21] Bacon, M., Shen, K. Y., and Cooper, J., Phys. Rev. **188**, 50 (1969).
[22] Bacon, M., to be published.
[23] Godfrey, T., Vidal, C. R., Cooper, J., and Smith, E. W., Phys. Rev., to be published.
[24] Huber, D. L., and VanVleck, J. H., Rev. Mod. Phys. **38**, 187 (1966).
[25] Sholin, G. V., Opt. Spectrosc. **26**, 275 (1969).
[26] Griem, H. R., Phys. Rev. **140**, A1140 (1965).
[27] Nguyen-Hoe, Drawin, H. W., and Herman, L., J. Quant. Spectr. Radiative Transfer **4**, 847 (1964).
[28] Vidal, C. R., Cooper, J., and Smith, E. W., Nat. Bur. Stand. (U.S.), Monogr. 116, 143 pages (May 1970).

8. Appendix. Program for Calculating the Line Profile $I(\Delta\omega)$

The program presented has been arranged in a very similar manner to the program given in Appendix C of the NBS Monograph [28], which was only able to calculate the Lyman lines. The first general version (program version A) is in principle able to compute any hydrogen line and is only limited by the available memory space of the computer. It has been written to calculate the Lyman lines up to $n = 16$, the Balmer lines up to $n = 8$ and the Paschen lines up to $n = 5$. By replacing the main program STBRHY and the function AIIM by the program STBRHY and the function AIIM listed in the end, the program may be simplified to calculate any hydrogen line neglecting lower state interaction (program version B). The arrays have been dimensioned such that the program is able to calculate all the Lyman, Balmer, and Paschen lines up to $n = 16$, As demonstrated in figure 1, this simplified version is completely adequate for all the Balmer lines beyond H_δ. For all the Lyman lines it is also noticeably faster than the first general version and the program given in Appendix C of the NBS Monograph.

1. The Fourier transform of the thermal average.

The function FOUTR calculates essentially the Fourier transform of the thermal average such that

$$\text{CCREAL} = \text{Re}\ \{i\Delta\omega_R^2 i(\Delta\omega_R, \beta, n, n', q_b, q_b', q_c, q_c')\} \tag{A1}$$

and

$$\text{CCIMAG} = Im\ \{i\Delta\omega_R^2 i(\Delta\omega_R, \beta, n, n', q_b, q_b', q_c, q_c')\} \tag{A2}$$

where

$$\text{DOM} = \Delta\omega_R = [\ \Delta\omega - \Delta\omega_i(n, q_b, n', q_b')\ \beta\ ]/\tilde{\omega}_p. \tag{A3}$$

In evaluating $i(\Delta\omega_R)$ according to eq (19) it computes $i(k=1, \Delta\omega_R)$ as defined in eq (20) and $i(k=2, \Delta\omega_R)$ as defined in eq (X.22) of paper I. The required Bessel functions J_0, J_1, Y_0 and Y_1 are obtained from the subroutine BSJY01. For large and small arguments $\Delta\omega_R$ the proper expansions are applied as discussed in paper I. The constants p_1, p_2 and $b_1(P1, P2, B1)$ specifying $i(k=1, \Delta\omega_R)$ and a_2 and $b_2(A2, B2)$ specifying $i(k=2, \Delta\omega_R)$ are set in the function AIIM and are calculated once for all the Stark components in the main program STBRHY.

2. The profile $I(\Delta\omega, \beta)$.

The function AIIM evaluates $I(\Delta\omega, \beta)$ as required by eq (1). The program is executed twice to obtain the contribution to $I(\Delta\omega, \beta)$ from the blocks of the K and $\mathscr{L}$-matrix with $M=0$ ($MBL=1$) and $M=\pm 1$ ($MBL=2$). It establishes first of all the $\mathscr{L}$-matrix according to eq (13). The necessary K-matrix (three dimensional array SLOP) as defined in eq (14) is read in or calculated once in the main program, while the Fourier transform $i(\Delta\omega_R)$ is obtained from the subroutine FOUTR described above. In order to reduce the size of the array SLOP the symmetry of the K-matrix with respect to the diagonal (see eq (28)) is used.

The matrix ordering is established once in the main program to allow for the partitioning discussed in section 3. The quantum numbers q_a, m_a, q'_a and m'_a are specified by the running index NRA, q_b, m_b, q'_b and m'_b by NRB and q_c and q'_c by NRC. Having set up the real and imaginary matrices of the operator $[\Delta\omega_{op}-\mathscr{L}(\Delta\omega_{op})]$ the imaginary part of the invers is determined according to eq (34) performing the matrix inversion by means of the subroutine ENVERS. The resulting matrix is then multiplied by the dipole matrix of eq (25), which is also calculated once in the main program such that

$$\mathrm{DIPOL}=(-1)^{\frac{1}{2}(n+n'-q-q'-M-2)}\quad (2l+1)(2l'+1)\langle nl|r|n'l'\rangle$$
$$\begin{pmatrix} \frac{n-1}{2} & \frac{n-1}{2} & l \\ \frac{m-q}{2} & \frac{m+q}{2} & -m \end{pmatrix}\begin{pmatrix} \frac{n'-1}{2} & \frac{n'-1}{2} & l' \\ \frac{m'-q'}{2} & \frac{m'+q'}{2} & -m' \end{pmatrix}\begin{pmatrix} l' & l & 1 \\ m' & -m & -M \end{pmatrix}\begin{pmatrix} l' & l & 1 \\ 0 & 0 & 0 \end{pmatrix} \tag{A4}$$

The function AIIM listed at the end for the case of no lower state interactions is arranged almost identically to the function AIIM just described. The only difference is that now the $\mathscr{L}$- and K-matrices are block diagonal in m, m' and q' according to eq (26) which allows a partitioning into smaller submatrices whose contribution to $I(\Delta\omega, \beta)$ is then again evaluated successively.

3. The final profile $I(\Delta\omega)$.

The main program STBRHY calculates the final line profile by performing the ion field average according to eq (1). It reads in first the low frequency component of the electric microfields [6, 7] for $0 < \beta \leq 30$ in steps of 0.1 for 5 different values of the shielding parameter $r_0/D=0., 0.2, 0.4, 0.6$ and 0.8. A listing of the distribution functions is given at the end of the program. (The deck of the distribution function was kindly supplied by Dr. C. F. Hooper.) The program then reads in the density n_e, the temperature T, the upper and lower state principal quantum numbers n and n', the initial value $\Delta\omega$, for which the line intensity is calculated, the logarithmic step width, the total number of points to be calculated, a parameter, which specifies the number of ion field integration points and finally 6 numbers, which specify the characteristic constants a_2 and b_2 of the G_2-function for all Stark components. These 6 numbers may be obtained from the calculations of the thermal average described in appendix A of the NBS Monograph. As shown, however, in paper I the contribution of the G_2-function can in practically all cases by neglected and hence one may set all 6 numbers to zero as done in this paper.

The program starts out to calculate the microfield distribution function for the particular shielding parameter as defined in eq (37) by using the 5 point interpolation subroutine POLY5 and stores the values in the array FIELD. It then calculates the average ion field

$$\beta_{av}=\int_0^\infty \beta W(\beta)\,d\beta \tag{A5}$$

by means of Weddle's rule (subroutine WEDDLE).

Next the program reads in a characteristic number NPUNCH. If this number is larger than 1

the program reads in the complete K-matrix (array SLOP) for the particular hydrogen line, which may have been obtained from another run of the program. Some numbers, which specify the size of the K-matrix, are read together with NPUNCH. If NPUNCH is smaller than 1 the program calculates the required K-matrix and if NPUNCH is equal to 1 it also punches the K-matrix out on cards. In the latter two cases the numbers NUR(1), NUR(2), IPI and NNCCQ, which specify the size of the K-matrix, may be set to any arbitrary value. The described feature was built into the program because the computation of the K-matrix may be very time consuming and is required only once for every hydrogen line as explained in section 3. It took, for example, on the CDC 3800 3 minutes to calculate the K-matrix of H_α, 8 minutes for H_β, 40 minutes for H_γ and 100 minutes for H_δ.

As a next step the program calculates the wavelength in standard air of the particular hydrogen line. It then calculates all the necessary radial matrix elements $\langle nl|r|n'l'\rangle$ by means of the function RADMAT, which in turn obtains the factorials from the function FCTRL. The values are stored in the array RDM according to

$$\mathrm{RDM}=\begin{pmatrix} l & l' & 1 \\ 0 & 0 & 0 \end{pmatrix}\langle nl|r|n'l'\rangle \tag{A6}$$

and the total line strength

$$\mathrm{STOT}=\sum_{l,l'}(2l+1)(2l'+1)\begin{pmatrix} l & l' & 1 \\ 0 & 0 & 0 \end{pmatrix}^2|\langle nl|r|n'l'\rangle|^2 \tag{A7}$$

is determined. The program then calculates all the necessary unitary transformations $\langle nlm|nqm\rangle$ as defined in eq (15) using the $3j$ symbol function S3J and stores them for the upper and lower states in the arrays SJUU and SJLL. With these transformations the dipol matrix elements between parabolic states are calculated and stored in the array DIPOL according to eq (A4). Simultaneously, the matrix ordering of the K- and $\mathscr{L}$-matrix is established such that the quantum numbers q, q', m and m' of a particular state $|nqm;n'q'm'\rangle$ are replaced by one running index NRUN and the block number MBLOCK, which may be 1 or 2 for $M=0$ and $M=\pm 1$ (see eq (29)). The values of the individual quantum numbers are stored in the arrays NQUU, NQLL, MMUU and MMLL.

The program then proceeds to calculate the K-matrix (array SLOP) according to eq (14) if NPUNCH is smaller or equal to 1 as explained above. Although the values for the eight different unitary transformations in eq (14) are stored, the computer time may still become rather long for the higher series members due to the extensive sumation over the quantum numbers l_a, l'_a, l_b, l'_b, L, m_c and m'_c.

As a last preliminary calculation the constants p_1, p_2, b_1, a_2, and b_2 for all the Stark components as required by the function AIIM for the subroutine FOUTR are determined and stored in the array FPAR. The constants p_2, a_1, and b_1 are evaluated for a lower cutoff $\rho_{\min}=\lambda+\frac{3}{2}n^2a_0$. As explained in the appendix of paper I the constant B in eqs (22) and (23) is obtained from

$$B=2-3\gamma-2\left[\frac{1-\cos(z)}{z^2}+\frac{\sin(z)}{z}-Ci(z)\right] \tag{A8}$$

where

$$z=3n_k\lambda/\rho_{\min} \tag{A9}$$

The necessary cosine integral is calculated by the function COSINT.

Finally the program is prepared to actually perform the ion field average. The distribution function $P(\beta)$ is obtained from the function *WFLD*, which uses a 5 point interpolation on the values initially stored in the array FIELD. For $\beta>30$ the function *WFLD* uses an asymptotic expansion. The ion field integral is performed by means of Weddle's rule (subroutine WEDDLE). The integrand is subdivided into several intervals depending on the spacing and the width of the individual Stark components. A convenient change of variables is used in every interval.
For

$$\Delta\omega>5\beta_{\mathrm{av}}\Delta\omega_i[(nq-n'q')_{\max}] \tag{A10}$$

the ion field integral is replaced by $I(\Delta\omega,\ \beta=\beta_{\mathrm{av}})$ as discussed in paper I. Besides the ion field integral the program calculates the wavelength perturbation $\Delta\lambda$ (DLAM), which corresponds to $\Delta\omega/\bar{\omega}_p$, the static profile for $N=n_e$ (FHOLTS), the asymptotic $\Delta\omega^{-5/2}$-wing (WING52), the one electron limit for $\beta=0$ (AWING), $I(\Delta\omega,\ \beta=0)$ and $I(\Delta\omega,\ \beta=\beta_{\mathrm{av}})$. The latter three values are printed out normalized with respect to the asymptotic $\Delta\omega^{-5/2}$-wing.

As explained above the program STBRHY may be replaced by the program STBRHY listed at the end for the case of no lower state interactions. Both programs are written in identically the same manner with the only difference that the program STBRHY listed at the end has a simpler matrix ordering and a much simpler and faster calculation of the K-matrix according to eq (27), which makes the provision to read in the K-matrix no longer desirable.

```
      PROGRAM STBRHY
C
C     PROGRAM FOR CALCULATING THE STARKBROADENING OF HYDROGEN ON THE
C     BASIS OF THE UNIFIED THEORY INCLUDING LOWER STATE INTERACTION
      DIMENSION DQQ(30),PFAC(6),STRONG(34),FF(1100),SJUU(136,31),
     1   SJLL(6,5),RDM(16,3),SLUU(16),SLLL(3),NQUU(34,2),NQLL(34,2),
     2   MMUU(34,2),MMLL(34,2),NQCU(30),NQCL(30),NXX(30),NST(30),
     3   DST(30),W(300,5)
      COMMON/FDAT/P1,P2,B1,A2,B2,PPFF,CCREAL,CCIMAG
      COMMON/PFW/FIELD(301)
      COMMON/11/SLOP(595,22,2)
      COMMON/22/DIPOL(34,2),NUR(2),IPI,NCQ,BET,FPAR(6,30),ADIFF(34,2),
     1   NSTEP
      COMMON/33/AMATR(34,68), BMATR(34,34), CMATR(34,34)
      EQUIVALENCE (SJUU,AMATR),(FF(601),NQUU),(FF(669),NQLL),
     1   (FF(737),MMUU),(FF(805),MMLL),(FF(873),NQCU),(FF(903),NQCL),
     2   (FF(933),SJLL),(FF(963),RDM),(FF(1011),SLUU),(FF(1027),STRONG)
      FIELD(1) = 0.0
      READ 100, ((W(I,J), J = 1,5), I = 1,300)
  100 FORMAT (5E12.4)
  120 READ 150, DEN,TEMP,NNUU,NNLL,GIN,DGG,NTOT,NFAC,(PFAC(I),I=1,6)
  150 FORMAT (2E10.2,I3,I2,2F10.2,2I5/6F10.5)
      IF (EOF,60) 577, 170
C     CALCULATION OF MICROFIELD DISTRIBUTION FUNCTION
  170 SHIELD = 0.0898 * DEN**(1./6.)/SQRT(TEMP)
      DO 161 J = 1,5
  161 DST(J) = 0.2 * FLOAT(J-1)
      DO 163 I = 1,300
      DO 162 J = 1,5
  162 DQQ(J) = W(I,J)
      CALL POLY5 (DST,DQQ,5,STRONG,SLUU,SHIELD,0.1,1)
  163 FIELD(I+1) = SLUU(1)
C     CALCULATION OF AVERAGE IONFIELD
      DO 111 I = 1,300
      AM = I
  111 FF(I) = FIELD(I+1) * AM/10.
      CALL WEDDLE (0.1,300,FF,BAV,0.)
      DY = 1./300.  $  Y = 0.
      DO 113 I = 1,10
      Y = Y + DY  $  B = 1./Y
  113 FF(I) = WFLD(B) * B**3
      CALL WEDDLE (DY,10,FF,DB,0.)
      BAV = BAV + DB
      READ 175,NPUNCH,(NUR(I),I=1,2),IPI,NNCCQ
  175 FORMAT (5I10)
C     FOR NPUNCH GT 1 K-MATRIX IS READ IN
C     FOR NPUNCH LT 1 K-MATRIX IS CALCULATED
C     FOR NPUNCH EQ 1 K-MATRIX IS CALCULATED AND PUNCHED OUT
      IF (NPUNCH.LE.1) GO TO 178
      DO 173 MBLOCK = 1,2
      NUPP = NUR(MBLOCK)
      NRRAB = (NUPP+1)*NUPP/2
      DO 174 J = IPI,NNCCQ
      READ 172, (FF(I),I=1,NRRAB)
  172 FORMAT (5E16.9)
      DO 171 I = 1,NRRAB
  171 SLOP(I,J,MBLOCK) = FF(I)
  174 CONTINUE
  173 CONTINUE
C     CALCULATION OF WAVELENGTH IN STANDARD AIR
  178 AUU = NNUU
      ALL = NNLL
      SL1 = 109678.758 * (1./(ALL*ALL) - 1./(AUU*AUU))
```

```
      SL2 = SL1 * SL1
      ALDD = 1.000064328+2949810./(1.46E+10-SL2)+25540./(4.1E+9-SL2)
      ALAM = 1.E+8/(ALDD * SL1)
      PRINT 180, DEN, TEMP, NNUU, NNLL, ALAM, SHIELD
 180  FORMAT (1H1,*  DENSITY =* E10.2* TEMPERATURE =*E10.2,
     1   * QUANTUMNUMBERS  N UPPER =*I3*  N LOWER =*I2* WAVELENGTH =*
     2   F8.2* ANGSTROM*/10X,*SHIELDING PARAMETER =*F6.3,10X,
     3   * INCLUDING LOWER STATE INTERACTION *//)
      IF (NNUU.LE.5.AND.NNLL.LE.3) GO TO 200
      IF (NNUU.LE.8.AND.NNLL.LE.2) GO TO 200
      IF (NNUU.LE.16.AND.NNLL.EQ.1) GO TO 200
      PRINT 190
 190  FORMAT (* OVERFLOW OF MATRICES, PROGRAM NOT EXECUTED*)
 577  CALL EXIT
C
C     RADIAL MATRIXELEMENTS AND TOTAL LINESTRENGTH
 200  IPI = 2
      STOT = 0.
      DO 330 KLL = 1,NNLL
      LLL = KLL - 1  $  ALL = LLL
      DO 310 KUU = 1,NNUU
      LUU = KUU - 1  $  AUU = LUU  $  RRMM = 0.
      IF (IABS(KUU - KLL).NE.1) GO TO 310
      RRMM = RADMAT(NNUU,LUU,NNLL,LLL) * S3J(ALL,AUU,1.,0.,0.,0.)
      STOT = STOT + (2.*ALL+1.)*(2.*AUU+1.) * RRMM * RRMM
 310  RDM(KUU,KLL) = RRMM
 330  CONTINUE
      SQST = SQRT(STOT)
C
C     TRANSFORMATION MATRICES
      DO 370 NKK = 1,2
      NN = NNLL
      IF (NKK.EQ.2) NN = NNUU
      ANN = NN  $  AN1 = 0.5 * (ANN - 1.)
      KQQ = 2 * NN - 1  $  NRUN = 0
      DO 370 KL = 1,NN
      AL = KL - 1
      FACC = SQRT(2.*AL+1.)
      IF(NKK.EQ.1) SLLL(KL) = FACC
      IF(NKK.EQ.2) SLUU(KL) = FACC
      DO 370 KM = 1,KL
      AM = KM - 1  $  NRUN = NRUN + 1
      QQ = -ANN  $  ALIM = ANN - 0.9 - AM
      DO 370 KQ = 1,KQQ
      QQ = QQ + 1.  $  SIIJ = 0.  $  ABQQ = ABS(QQ)
      IF (ABQQ.GT.ALIM) GO TO 360
      NQ = ABQQ + 0.1
      IF (MOD(NN+NQ+KM+1,2).NE.1) GO TO 360
      AMQ = 0.5 * (AM - QQ)  $  APQ = 0.5 * (AM + QQ)
      SIIJ = FACC * S3J(AN1,AN1,AL,AMQ,APQ,-AM)
 360  IF (NKK.EQ.1) SJLL(NRUN,KQ) = SIIJ
      IF (NKK.EQ.2) SJUU(NRUN,KQ) = SIIJ
 370  CONTINUE
C
C     DIPOLMATRIXELEMENTS IN PARABOLIC STATES AND MATRIX ORDERING
      KQUU = 2 * NNUU - 1  $  KQLL = 2 * NNLL - 1
      DO 500 MBLOCK = 1,2
      AMLCK = MBLOCK  $  MBL = MBLOCK - 1  $  AMBL = MBL
      NRUN = 0  $  NCQ = 0  $  NAQU = -NNUU
      DO 480 KUU = 1,KQUU
      NAQU = NAQU + 1  $  KQU = NNUU + NAQU  $  NAQL = -NNLL
      DO 480 KLL = 1,KQLL
      NAQL = NAQL + 1
```

```
      KQL = NNLL + NAQL
      NXDIF = NNUU * NAQU - NNLL * NAQL
      AXDIF = NXDIF
      IF (NXDIF.LT.0) GO TO 400
      NCQ = NCQ + 1
      IF (MBLOCK.EQ.2) GO TO 400
      NQCU(NCQ) = NAQU  $  NQCL(NCQ) = NAQL
      NXX(NCQ) = NXDIF  $  DQQ(NCQ) = 0.
  400 NPHAS = (NNUU + NNLL + MBL - NAQU - NAQL - 2)/2
      PHASE = (-1.)**MOD(NPHAS,2)
      KMINL = NNLL - IABS(NAQL)  $  KMINU = NNUU - IABS(NAQU)
      KML = -KMINL  $  MKML = 2 * KMINL - 1
      DO 470 KAML = 1,MKML
      KML = KML + 1
      IF (MOD(NNLL+NAQL+KML,2).NE.1) GO TO 470
      KMU = KML + MBL
      IF (IABS(KMU).GE.KMINU) GO TO 470
      IF (MOD(NNUU+NAQU+KMU,2).NE.1) GO TO 470
      NRUN = NRUN + 1
      NQUU(NRUN,MBLOCK) = NAQU  $  NQLL(NRUN,MBLOCK) = NAQL
      MMUU(NRUN,MBLOCK) = KMU  $  MMLL(NRUN,MBLOCK) = KML
      ADIFF(NRUN,MBLOCK) = AXDIF
      AMU = KMU  $  AML = KML
      KBBU = IABS(KMU) + 1  $  KBBL = IABS(KML) + 1
      RESULT = 0.
      DO 450 KKLU = KBBU,NNUU
      ALU = KKLU - 1
      LLU = (KKLU-1) * KKLU / 2 + KBBU
      FAC1 = SLUU(KKLU) * SJUU(LLU,KQU)
      DO 450 KKLL = KBBL,NNLL
      IF (IABS(KKLU - KKLL).NE.1) GO TO 450
      ALL = KKLL - 1
      LLL = (KKLL - 1) * KKLL / 2 + KBBL
      FAC2 = SLLL(KKLL) * SJLL(LLL,KQL)
      FACC = FAC2 * FAC1 * S3J(ALL,ALU,1.,AML,-AMU,AMBL)
      RESULT = RESULT + FACC * RDM(KKLU,KKLL)
  450 CONTINUE
      SIIJ = RESULT * PHASE / SQST
      DIPOL(NRUN,MBLOCK) = SIIJ
      IF (NXDIF.GE.0) DQQ(NCQ) = DQQ(NCQ) + AMLCK*RESULT*RESULT/STOT
      PRINT 425,NAQU,KMU,NAQL,KML,SIIJ
  425 FORMAT (16X,*(*,2I3,*  I D I*,2I3,* )  =*E16.8)
  470 CONTINUE
  480 CONTINUE
      NUR(MBLOCK) = NRUN
      PRINT 393
  393 FORMAT(/)
  500 CONTINUE
C
C     REORDERING OF THE STARK COMPONENTS
      NCM1 = NCQ - 1
      DO 333 II = 1,NCM1
      IPP = II + 1
      DO 333 JJ = IPP,NCQ
      IF (NXX(II).LE.NXX(JJ)) GO TO 333
      TEMPP = NXX(II)  $  NXX(II) = NXX(JJ)  $  NXX(JJ) = TEMPP
      TEMPP = DQQ(II)  $  DQQ(II) = DQQ(JJ)  $  DQQ(JJ) = TEMPP
      TEMPP = NQCU(II)  $  NQCU(II) = NQCU(JJ)  $  NQCU(JJ) = TEMPP
      TEMPP = NQCL(II)  $  NQCL(II) = NQCL(JJ)  $  NQCL(JJ) = TEMPP
  333 CONTINUE
      PRINT 410, (NQCU(I),NQCL(I),NXX(I),DQQ(I), I = 1,NCQ)
  410 FORMAT (15X,* Q UPPER =*I3,* Q LOWER =*I3,* X =*I5,* DIPOL=*E16.8)
```

```
      PRINT 393
      JJ = 1  $  KMST = 0
  315 KMST = KMST + 1
      DST(KMST) = 0.
      DO 325 II = JJ,NCQ
      IF (NXX(II).NE.NXX(JJ)) GO TO 325
      NST(KMST) = NXX(II)  $  DST(KMST) = DST(KMST) + DQQ(II)
      J = II
  325 CONTINUE
      JJ = J + 1
      IF (JJ.GT.NCQ) GO TO 345
      GO TO 315
  345 PRINT 355, (NST(I),DST(I),I = 1,KMST)
  355 FORMAT (16X,*X =*I3,F20.10)
      PRINT 393
C
C     K OPERATOR MATRIX
      IF (NPUNCH-1) 445,455,650
  455 IPP = 2
      PUNCH 465,IPP,(NUR(I),I=1,2),IPI,NCQ,NNUU,NNLL
  465 FORMAT (5I10,15X,2I5)
  445 NTIME = KLOCK(0)
      DO 600 MBLOCK = 1,2
      MBL = 1 - MBLOCK  $  AMBL = MBL  $  NUPP = NUR(MBLOCK)
      DO 600 NRC = IPI,NCQ
      NCQU = NQCU(NRC)  $  NCQL = NQCL(NRC)
      KCQU = NNUU + NCQU  $  KCQL = NNLL + NCQL
      IMULIM = NNUU - IABS(NCQU)  $  IMLLIM = NNLL - IABS(NCQL)
      DO 590 NRA = 1,NUPP
      NAQU = NQUU(NRA,MBLOCK)  $  KAMU = MMUU(NRA,MBLOCK)
      AMU = KAMU  $  IABAMU = IABS(KAMU)
      NAQL = NQLL(NRA,MBLOCK)  $  KAML = MMLL(NRA,MBLOCK)
      AML = KAML  $  IABAML = IABS( KAML)
      KAQU = NNUU + NAQU  $  KAQL = NNLL + NAQL
      KAAU = IABS(KAMU) + 1  $  KAAL = IABS(KAML) + 1
      DO 580 NRB = 1,NRA
      NRRAB = (NRA - 1) * NRA / 2 + NRB
      NBQU = NQUU(NRB,MBLOCK)  $  KBMU = MMUU(NRB,MBLOCK)
      BMU = KBMU  $  IABBMU = IABS(KBMU)
      NBQL = NQLL(NRB,MBLOCK)  $  KBML = MMLL(NRB,MBLOCK)
      BML = KBML  $  IABBML = IABS(KBML)
      KBQU = NNUU + NBQU  $  KBQL = NNLL + NBQL
      KBBU = IABS(KBMU) + 1  $  KBBL = IABS(KBML) + 1
      NPHAS = MBL - NCQU - NCQL - (NAQU+NAQL+NBQU+NBQL)/2
      SIIJ = 0.
      DO 540 JLAL = KAAL,NNLL
      ALL = JLAL - 1
      LALL = (JLAL - 1) * JLAL / 2 + IABAML + 1
      FAC1 = SJLL(LALL,KAQL)
      DO 540 JLAU = KAAU,NNUU
      ALU = JLAU - 1
      LALU = (JLAU - 1) * JLAU / 2 + IABAMU + 1
      FAC2 = SJUU(LALU,KAQU)  $  FAC12 = FAC1 * FAC2
      DO 540 JLBL = KBBL,NNLL
      BLL = JLBL - 1
      LBLL = (JLBL - 1) * JLBL / 2 + IABBML + 1
      FAC3 = SJLL(LBLL,KBQL)  $  FAC13 = FAC12 * FAC3
      MCLUP = MINO(JLBL,JLAL) - 1
      DO 540 JLBU = KBBU,NNUU
      BLU = JLBU - 1
      LBLU = (JLBU - 1) * JLBU / 2 + IABBMU + 1
      FAC4 = SJUU(LBLU,KBQU)  $  FAC14 = FAC13 * FAC4
      MCUUP = MINO(JLBU,JLAU) - 1
```

```
      IUPP = MIN0(IABS(JLAU+JLAL),IABS(JLBU+JLBL)) - 1
      MCL = -IMLLIM - 1
      DO 540 JMCLL = 1,IMLLIM
      MCL = MCL + 2  $  IABCML = IABS(MCL)
      IF (IABCML.GT.MCLUP) GO TO 540
      AMCL = MCL
      LALL = (JLAL - 1) * JLAL / 2 + IABCML + 1
      LBLL = (JLBL - 1) * JLBL / 2 + IABCML + 1
      FAC5 = SJLL(LALL,KCQL) * SJLL(LBLL,KCQL)
      FAC15 = FAC14 * FAC5
      IF (ABS(FAC15).LT.1.E-8) GO TO 540
      MCU = -IMULIM - 1
      DO 535 JMCUU = 1,IMULIM
      MCU = MCU + 2  $  IABCMU = IABS(MCU)
      IF (IABCMU.GT.MCUUP) GO TO 535
      AMCU = MCU
      LALU = (JLAU - 1) * JLAU / 2 + IABCMU + 1
      LBLU = (JLBU - 1) * JLBU / 2 + IABCMU + 1
      FAC6 = SJUU(LALU,KCQU) * SJUU(LBLU,KCQU)
      IF (ABS(FAC6).LT.1.E-8) GO TO 535
      MGGL = MCL - MCU  $  AMGL = MGGL
      ILOW = MAX0(MBL,IABS(MGGL),IABS(JLAU-JLAL),IABS(JLBU-JLBL)) + 1
      IF (ILOW.GT.IUPP) GO TO 535
      FAC16 = FAC15 * FAC6 * ((-1.)**MOD(NPHAS-MGGL,2))
      DO 530 JLDD = ILOW,IUPP
      IF (MOD(JLAL+JLAU+JLDD,2).NE.0) GO TO 515
      IF (KAMU.EQ.0.AND.KAML.EQ.0) GO TO 530
      IF (MCL.EQ.0.AND.MCU.EQ.0) GO TO 530
 515  IF (MOD(JLBL+JLBU+JLDD,2).NE.0) GO TO 520
      IF (KBMU.EQ.0.AND.KBML.EQ.0) GO TO 530
      IF (MCL.EQ.0.AND.MCU.EQ.0) GO TO 530
 520  ALDD = JLDD - 1
      FAC7 = S3J(ALL,ALU,ALDD,-AMCL,AMCU,AMGL) * (2.*ALDD + 1.)
      FAC7 = FAC7 * S3J(ALL,ALU,ALDD,-AML,AMU,AMBL)
      FAC7 = FAC7 * S3J(BLL,BLU,ALDD,-AMCL,AMCU,AMGL)
      FACC = FAC7 * S3J(BLL,BLU,ALDD,-BML,BMU,AMBL) * FAC16
      SIIJ = SIIJ + FACC
 530  CONTINUE
 535  CONTINUE
 540  CONTINUE
      SLOP(NRRAB,NRC,MBLOCK) = SIIJ
 580  FF(NRRAB) = SIIJ
 590  CONTINUE
      IF (NPUNCH.EQ.1) PUNCH 630,(FF(I),I=1,NRRAB)
 630  FORMAT (5E16.9)
 600  CONTINUE
      NTIME = -NTIME + KLOCK(0)
      PRINT 617, NTIME
 617  FORMAT (16X,*COMPUTERTIME FOR CALCULATING K-OPERATOR MATRIX =*I8/)
C
C     BASIC CONSTANTS AND ARRAY FOR G-FUNCTION CONSTANTS
 650  SDEN = SQRT(DEN)
      FAC = 2064.936 * TEMP * SQRT(TEMP/DEN)
      CFAC = 4.5645E-7 * SDEN/TEMP
      DEBROG = 2.1027E-6/SQRT(TEMP)
      ANN = NNUU
      RMIN = DEBROG + ANN * ANN * 7.9376E-9
      BET = 5.6558E-5 * DEN**(1./6.)
      ASY = 0.0
      DO 270 NRC = IPI,NCQ
      QC = NXX(NRC)  $  C = CFAC * QC
      P1 = -1.671086 * FAC * C * SQRT(C)
      BS = 3. * QC * DEBROG / RMIN
```

```
      STRONG(NRC) = 0.269-2.*(((1.-COSF(BS))/BS+SINF(BS))/BS-COSINT(BS))
      PPFF = -1.128379 * FAC * C * C
      P2 = PPFF * (STRONG(NRC)-2.*LOGF(2.*C))
      FPAR(1,NRC) = P1  $  FPAR(2,NRC) = P2
      FPAR(3,NRC) = 0.5 * (P2/P1)**2  $  FIN = LOGF(QC)
      A2 = P2*((PFAC(3)*FIN+PFAC(2))*FIN+PFAC(1))
      B2 = (PFAC(6)*FIN+PFAC(5))*FIN + PFAC(4)
      IF (B2.LT.0.) A2 = 0.
      FPAR(4,NRC) = A2  $  FPAR(5,NRC) = B2  $ FPAR(6,NRC) = PPFF
  270 ASY = ASY + 2. * P1 * DQQ(NRC)
      PRINT 220
  220 FORMAT (/13X*P1*18X*P2*18X*B1*18X*A2*18X*B2*17X*STRONG*/)
      PRINT 240,((FPAR(K,I),K = 1,5),STRONG(I), I = IPI,NCQ)
  240 FORMAT (6E20.4)
      PRINT 280, FAC, CFAC, BET, ASY, DEBROG, BAV, NFAC
  280 FORMAT(/* FAC =*E11.4,* CFAC =*E11.4,* BET =*E11.4,* ASY =*E11.4,
     1   * DEBROG =*E11.4,* BAV =*F7.4,* INTEGRATIONFACTOR =*I2//
     2   5X*DOM*8X*DLAM*8X*ITOT*6X*IHOLTS*8X*ASY*10X*WING*7X*WHOLTS*7X,
     3   *WW00*8X*WWBB*8X*WWNG*8X*TIME  STEPS*/)
      ADLFAC = 4.23538E-15 * SDEN * ALAM * ALAM
C
C     CALCULATION OF THE IONFIELD INTEGRAL
      N12 = 12 * NFAC  $  AN12 = N12  $  N30 = 30 * NFAC  $  AN30 = N30
      DMCRT = BET * BAV * NXX(NCQ) * 5.
      G = GIN - DGG
      DO 950 MM = 1,NTOT
      NTIME = KLOCK(0)
      NSTEP = 0  $  G = G + DGG
      DOM = 10. ** G  $  DLAM = ADLFAC * DOM
      WING52 = -0.2992067103 * ASY/(SQRT(DOM) * DOM * DOM)
      FHOLTS = 0.  $  AWING = 0.
      DO 815 NRC = IPI,NCQ
      P1 = FPAR(1,NRC)  $  P2 = FPAR(2,NRC)  $  B1 = FPAR(3,NRC)
      A2 = FPAR(4,NRC)  $  B2 = FPAR(5,NRC)  $  PPFF = FPAR(6,NRC)
      CALL FOUTR(DOM)
      AWING = AWING + DQQ(NRC) * CCIMAG * 2./(DOM*DOM)
      QC = NXX(NRC)  $  BETFAC = BET * QC  $  BCRIT = DOM/BETFAC
  815 FHOLTS = FHOLTS + DQQ(NRC) * WFLD(BCRIT) / BETFAC
      IF (DOM.GT.DMCRT) GO TO 985
      AIRES = 0.
      IF(DOM.GT.(-3.*P2)) GO TO 840
      ANQ1 = NXX(NCQ)
      BCRIT = (DOM - P2)/(ANQ1*BET)
      DB = BCRIT/AN12  $  B = 0.
      DO 820 J = 1,N12
      B = B + DB
  820 FF(J) = AIIM(DOM,B) * WFLD(B)
      CALL WEDDLE (DB,N12,FF,AIII,0.)
      AIRES = AIII
      DY = 1./(BCRIT*AN30)  $  Y = 0.
      DO 830 J = 1,N30
      Y = Y + DY  $  B = 1./Y
  830 FF(J) = B * B * AIIM(DOM,B) * WFLD(B)
      CALL WEDDLE (DY,N30,FF,AIII,0.)
      AIRES = AIRES + AIII
      GO TO 980
  840 BCRCR = DOM/BET
      EPSPS = -P2/BET
      DO 957 NQ = IPI,KMST
      ANQ = NST(NQ)
      BCR = BCRCR/ANQ  $  EPS = EPSPS/ANQ
      IF (NQ.EQ.IPI) GO TO 907
      SL1 = 1./(GAM - BCR)
```

```
      GO TO 908
907   SL1 = 0.
908   SL2 = 1./EPS
      SL3 = 1./(BCR + EPS)  $  SL4 = 1./(BCR - EPS)
      IF (NQ.EQ.KMST) GO TO 911
      ANQ1 = NST(NQ+1)
      GAM = 0.5 * (BCR-EPS+(BCRCR+EPSPS)/ANQ1)
      GO TO 912
911   GAM = 0.5 * (BCR-EPS)
912   SL5 = 1./(BCR-GAM)
      CRIT = SL2 - SL5
904   Y = SL1
      IF (NQ.EQ.IPI) GO TO 913
      B = BCR + 1./Y
      FA = AIIM(DOM,B) * WFLD(B)/(Y * Y)
      GO TO 914
913   FA = 0.
914   DY = (SL2 - SL1)/AN12
      DO 917 J = 1,N12
      Y = Y + DY  $  Y1 = 1./Y  $  B = BCR + Y1
917   FF(J) = Y1 * Y1 * AIIM(DOM,B) * WFLD(B)
      CALL WEDDLE (DY,N12,FF,AIII,FA)
      AIRES = AIRES + AIII
      Y = SL3  $  B = 1./Y
      FA = B * B * AIIM(DOM,B) * WFLD(B)
      DY = (SL4 - SL3)/AN12
      DO 927 J = 1,N12
      Y = Y + DY  $  B = 1./Y
927   FF(J) = B * B * AIIM(DOM,B) * WFLD(B)
      CALL WEDDLE (DY,N12,FF,AIII,FA)
      AIRES = AIRES + AIII
      IF(CRIT.LE.0.) GO TO 977
      Y = SL5  $  B = BCR - 1./Y
      FA = AIIM(DOM,B) * WFLD(B)/(Y * Y)
      DY = CRIT/AN12
      DO 937 J = 1,N12
      Y = Y + DY  $  Y1 = 1./Y  $  B = BCR - Y1
937   FF(J) = Y1 * Y1 * AIIM(DOM,B) * WFLD(B)
      CALL WEDDLE (DY,N12,FF,AIII,FA)
      AIRES = AIRES + AIII
957   CONTINUE
      IF(GAM.LT. 5.) GO TO 968
      Y = 1./GAM  $  DY = (0.2 - Y)/AN12
      FA = GAM * GAM * AIIM(DOM,GAM) * WFLD(GAM)
      DO 967 J = 1,N12
      Y = Y + DY  $  B = 1./Y
967   FF(J) = B * B * AIIM(DOM,B) * WFLD(B)
      CALL WEDDLE (DY,N12,FF,AIII,FA)
      AIRES = AIRES + AIII
      SL4 = 0.2
      GO TO 977
968   SL4 = 1./GAM
977   B = 0.
      DB = 1./(SL4 * AN30)
      DO 947 J = 1,N30
      B = B + DB
947   FF(J) = AIIM(DOM,B) * WFLD(B)
      CALL WEDDLE (DB,N30,FF,AIII,0.)
      AIRES = AIRES + AIII
980   WWBB = (AIIM(DOM,BAV) + FHOLTS)/WING52
      GO TO 990
985   AIRES = AIIM(DOM,BAV) + FHOLTS
      WWBB = 0.
```

```
 990  WING = AIRES/WING52
      WINHOL = FHOLTS/WING52
      WWOO = (AIIM(DOM, 0.) + FHOLTS)/WING52
      WWNG = (AWING + FHOLTS)/WING52
      NTIME = -NTIME + KLOCK(0)
 950  PRINT 978,DOM,DLAM,AIRES,FHOLTS,WING52,WING,WINHOL,WWOO,WWBB,
     1   WWNG,NTIME,NSTEP
 978  FORMAT (10E12.4,I10,I6)
      GO TO 120
      END
C
C
      FUNCTION AIIM(DOM,B)
C
C     CALCULATION OF I(DOM,B) FOR THE GENERAL CASE INCLUDING LOWER
C     STATE INTERACTION
      DIMENSION DRRF(34), DIIF(34), FMATR(34,34)
      COMMON/FDAT/P1,P2,B1,A2,B2,PPFF,CCREAL,CCIMAG
      COMMON/11/SLOP(595,22,2)
      COMMON/22/DIPOL(34,2),NUR(2),IPI,NCQ,BET,FPAR(6,30),ADIFF(34,2),
     1   NSTEP
      COMMON/33/AMATR(34,68), BMATR(34,34), CMATR(34,34)
      AIIM = 0.  $  NSTEP = NSTEP + 1
      DO 800 MBL = 1,2
      AML = MBL  $  NUPP = NUR(MBL)
      DO 750 NRB = 1,NUPP
      DOMRB = DOM - BET * B * ADIFF(NRB,MBL)
      DO 220 NRC = IPI,NCQ
      P1 = FPAR(1,NRC)  $  P2 = FPAR(2,NRC)  $  B1 = FPAR(3,NRC)
      A2 = FPAR(4,NRC)  $  B2 = FPAR(5,NRC)  $  PPFF = FPAR(6,NRC)
      CALL FOUTR(DOMRB)
      DRRF(NRC) = CCREAL
 220  DIIF(NRC) = CCIMAG
      DO 700 NRA = 1,NUPP
      IF (NRA.LE.NRB) NRRAB = (NRB - 1) * NRB / 2 + NRA
      IF (NRA.GT.NRB) NRRAB = (NRA - 1) * NRA / 2 + NRB
      ARRR = 0.  $  AIII = 0.
      DO 600 NRC = IPI,NCQ
      TEMP = SLOP(NRRAB,NRC,MBL)
      ARRR = ARRR + TEMP * DRRF(NRC)
 600  AIII = AIII + TEMP * DIIF(NRC)
      AIII = AIII * 6.2831853072
      AMATR(NRB,NRA) = AIII  $  CMATR(NRB,NRA) = AIII
 700  BMATR(NRB,NRA) = ARRR * 6.2831853072
 750  BMATR(NRB,NRB) = BMATR(NRB,NRB) + DOMRB
      CALL ENVERS (NUPP)
      DO 320 NRB = 1,NUPP
      DO 320 NRA = 1,NUPP
      TEMP = 0.
      DO 300 NRC = 1,NUPP
 300  TEMP = TEMP + BMATR(NRB,NRC) * AMATR(NRC,NRA+NUPP)
 320  FMATR(NRB,NRA) = TEMP
      DO 420 NRB = 1,NUPP
      DO 420 NRA = 1,NUPP
      TEMP = 0.
      DO 400 NRC = 1,NUPP
 400  TEMP = TEMP + FMATR(NRB,NRC) * BMATR(NRC,NRA)
 420  AMATR(NRB,NRA) = TEMP + CMATR(NRB,NRA)
      CALL ENVERS (NUPP)
      DO 795 NRB = 1,NUPP
      DO 795 NRA = 1,NUPP
 795  AIIM = AIIM+AML*DIPOL(NRB,MBL)*DIPOL(NRA,MBL)*AMATR(NRB,NRA+NUPP)
 800  CONTINUE
```

```
      AIIM =  AIIM * 0.3183099  $  RETURN
      END
C
C
      SUBROUTINE POLY5 (X,Y,NUMX,XN,YN,XNI,DX,NXNUM)
C     A 5 POINT POLYNOMIAL INTERPOLATION ROUTINE
C     FOR EACH POINT TO BE INTERPOLATED8 THE 5 NEAREST KNOWN POINTS
C     ARE CHOSEN, AND A 5TH DEGREE POLYNOMIAL IS FITTED TO THESE POINTS
C     X AND Y ARE THE ARRAYS OF KNOWN POINTS ON THE CURVE
C     NUMX IS THE NUMBER OF KNOWN POINTS
C     TWO NEW ARRAYS, XN AND YN WILL BE GENERATED FOR THE NXNUM VALUES
C     OF X AND F(X) STARTING WITH X=XNI IN INCREMENTS OF DX
      DIMENSION X(5),Y(5),XN(5),YN(5)
      J=2
      DO 8 I=1,NXNUM
      EYE=I-1
      XN(I)=XNI+DX*EYE
      IF (XN(I)-X(1)) 1,2,3
 2    YN(I)=Y(1)
      GO TO 8
 3    IF (XN(I).LE.X(J)) GO TO 4
      IF (J.GE.NUMX) GO TO 7
      J = J + 1
      GO TO 3
 1    L = 1
      GO TO 70
 7    L = NUMX - 4
      GO TO 70
 4    L = J - 1
      IF (J.GT.2) L = J - 2
      IF (J.GT.3) L = J - 3
      IF ((J+1).GT.NUMX) L = J - 4
 70   YN(I)=0.0
      LLL=L+4
      DO 75 K=L,LLL
      TERM=1.0
      DO 74 M=L,LLL
      IF (K.EQ.M) GO TO 74
      TDEN=X(K)-X(M)
      TNUM=XN(I)-X(M)
      TERM=TERM*TNUM/TDEN
 74   CONTINUE
      TERM=Y(K)*TERM
 75   YN(I)=YN(I)+TERM
 8    CONTINUE
      RETURN
      END
C
C
      SUBROUTINE FOUTR (DOM)
C
C     FOURIERTRANSFORM OF THERMAL AVERAGE FOR UNIFIED THEORY
      COMMON/FDAT/P1,P2,B1,A2,B2,PPFF,CCREAL,CCIMAG
      ARG = ABSF(DOM)
      Z = B1 * ARG
      IF (Z.LE.0.001) GO TO 600
      AR2 = ARG * ARG
      IF (Z.LE.40.) GO TO 300
      FAC1 = -0.2992067103 * P1/(SQRT(ARG) * AR2)
      CC = FAC1 * ((1. - 1.3125/Z)*0.625/Z + 1.)
      SS = CC - FAC1 * 1.25/Z
      GO TO 500
 300  CALL BSJY01 (Z, AJ0, Y0, AJ1, Y1)
```

```
      FAC1 = Y1/(2.*Z) + AJ1 - Y0
      FAC2 = AJ0 + Y1 - AJ1/(2.*Z)
      CINE = COSF(Z)
      SINE = SINF(Z)
      FCC = P2 * B1 * B1
      CC = FCC * (CINE*FAC1+SINE*FAC2)
      SS = FCC * (CINE*FAC2-SINE*FAC1)
      IF (A2.EQ.0.) GO TO 500
      Z = B2 * ARG
      IF (Z.GT.10.) GO TO 400
      CALL BSJY01 (Z, AJ0, Y0, AJ1, Y1)
      FAC1 = ((AJ1-Y0)*16.*Z-36.*AJ0-28.*Y1)*Z+15.*Y0-3.*AJ1
      FAC2 = ((AJ0+Y1)*16.*Z-36.*Y0+28.*AJ1)*Z-15.*AJ0-3.*Y1
      CINE = COSF(Z)
      SINE = SINF(Z)
      FCC = A2 * B2/6.
      CC = CC + FCC * (CINE*FAC1+SINE*FAC2)
      SS = SS + FCC * (CINE*FAC2-SINE*FAC1)
      GO TO 500
 400  FAC1 = 0.1322319336 * A2 * B2 * Z**(-3.5)
      FCC = FAC1 * (1. - (3.9375/Z + 1.)*4.375/Z)
      CC = CC + FCC
      SS = SS - FCC - FAC1*8.75/Z
 500  IF (DOM.LT.0.) SS = -SS
      CCREAL = -AR2 * SS
      CCIMAG =  AR2 * CC
      RETURN
 600  CCREAL =  0.3183099 * (P2*B1-A2) * DOM
      CCIMAG = -0.3183099 * P2
      RETURN
      END
C
C
      SUBROUTINE ENVERS (NN)
C
      COMMON/33/C(34,68),   BMATR(34,34),CMATR(34,34)
      N = NN
      IF (N.GT.1) GO TO 10
      C(1,2) = 1./C(1,1)
      RETURN
 10   DO 300 K = 1,N
      KN = K + N
      NP = KN - 1
      KP1 = K + 1
      TEMP = 1./C(K,K)
      DO 100 I = KP1,NP
 100  C(K,I) = C(K,I) * TEMP
      C(K,KN) = TEMP
      DO 300 L = 1,N
      IF (K.EQ.L) GO TO 300
      TEMP = C(L,K)
      DO 200 I = KP1,NP
 200  C(L,I) = C(L,I) - C(K,I) * TEMP
      C(L,KN) = -C(K,KN) * TEMP
 300  CONTINUE
      RETURN
      END
C
C
      FUNCTION RADMAT(N1,L1,N2,L2)
C
      DIMENSION F(2)
      RADMAT = 0.0
```

```
      IF(IABS(L1 - L2).NE.1) RETURN
      NA = N1  $  NB = N2  $  L = L1
      IF(L1.GT.L2) GO TO 10
      NA = N2  $  NB = N1  $  L = L2
   10 ANA = NA
      BNB = NB  $  AL = L
      IF(N1.EQ.N2) GO TO 60
      RADMAT = FCTRL(ANA + AL) * FCTRL(BNB + AL - 1.)
      RADMAT = RADMAT/(FCTRL(ANA - AL - 1.) * FCTRL(BNB - AL))
      RADMAT = SQRT(RADMAT)
      I = BNB + AL  $  AL = 2. * AL
      RADMAT = RADMAT * ((-1.0)**XMODF(I,2))/(4.*FCTRL(AL - 1.))
      ABAB = (ANA - BNB)/(ANA + BNB)
      AB2 = 1./(ANA - BNB)**2
      RADMAT = RADMAT * ABAB**(NA+NB)*(4.*ANA*BNB*AB2)**(L+1)
      Z = -4. * ANA * BNB * AB2
      NR = NA - L - 1  $  NRP = NB - L  $  ANRP = NRP
      DO 30 MM = 1,2
      F(MM) = 1.0
      IF(MM.EQ.2) NR = NR + 2
      K = MINO (NR,NRP)
      IF(K.EQ.0) GO TO 30
      ANR = NR  $  PROD = 1.0
      DO 40 M = 1,K
      AM = M - 1
      PROD = PROD * (AM-ANR)*(AM-ANRP)*Z/((AL+AM)*(AM+1.))
   40 F(MM) = F(MM) + PROD
   30 CONTINUE
      RADMAT = RADMAT * (F(1) - ABAB * ABAB * F(2))
      RETURN
   60 RADMAT = -1.5 * ANA * SQRT((ANA+AL)*(ANA-AL))
      RETURN
      END
C
C
      FUNCTION FCTRL(A)
C
C     CALCULATION OF FACTORIALS
      DIMENSION FCTI(20)
      DATA ((FCTI(I),I=1,20) =1.0,2.0,6.0,24.0,120.0,720.0,5040.0,
     1  40320.0,362880.0,3628800.0,39916800.0,479001600.0,
     2  6227020800.0,87178291200.0,1307674368000.0,
     3  2.0922789888E13, 3.55687428096E14, 6.402373705728E15,
     4  1.2164510040883 E17, 2.4329020081766 E18)
      I = A + 0.1
      IF(I) 50,60,70
 50   FCTRL = 0.0
      RETURN
 60   FCTRL = 1.0
      RETURN
 70   IF (I.GT.20) GO TO 130
      FCTRL=FCTI(I)
      RETURN
 130  F=20.0
      FCTRL=FCTI(20)
      DO 131 J=21,I
      F=F+1.0
 131  FCTRL=FCTRL*F
      RETURN
      END
C
C
      FUNCTION S3J (FJ1, FJ2, FJ3, FM1, FM2, FM3)
```

```
C
C     CALCULATION OF 3J-SYMBOL, FJ1+FJ2+FJ3 HAS TO BE LESS THAN 38
      DIMENSION  GAM(39)
      DATA  ((GAM(I),I=1,39) =1.,1.,2.,6.,24.,120.,720.,5040.,40320.,
     1   362880.,3628800.,39916800.,479001600.,6227020800.,87178291200.,
     2   1307674368000.,2.0922789888E+13,3.5568742810E+14,
     3   6.4023737057E+15,1.2164510041E+17,2.4329020082E+18,
     4   5.1090942172E+19,1.1240007278E+21,2.5852016739E+22,
     5   6.2044840173E+23,1.5511210043E+25,4.0329146113E+26,
     6   1.0888869450E+28,3.0488834461E+29,8.8417619937E+30,
     7   2.6525285981E+32,8.2228386542E+33,2.6313083693E+35,
     8   8.6833176188E+36,2.9523279904E+38,1.0333147966E+40,
     9   3.7199332679E+41,1.3763753091E+43,5.2302261747E+44)
      S3J=0.0
      FJA = FJ1+0.001 $ FJB = FJ2+0.001 $ FJC = FJ3+0.001
      IF (FJA.LT.0.0.OR.FJB.LT.0.0.OR.FJC.LT.0.0) RETURN
      IF (AMOD(FJA,0.5).GT.0.002) RETURN
      IF (AMOD(FJB,0.5).GT.0.002) RETURN
      IF (AMOD(FJC,0.5).GT.0.002) RETURN
      FMA = FM1 $ FMB = FM2 $ FMC = FM3
      IF (ABS(FMA).GT.FJA.OR.ABS(FMB).GT.FJB.OR.ABS(FMC).GT.FJC) RETURN
      B = FJA-FMA $ P = FJB-FMB $ D = FJC-FMC $ G = FJA+FJB-FJC
      IF ((ABS(FMA+FMB+FMC)+AMOD(B,1.)+AMOD(P,1.)+AMOD(D,1.)+DIM(0.,G)
     1   +DIM(ABS(FJA-FJB),FJC)).GT.0.01) RETURN
      IHH = FJA + FJB + FJC + 2.
      IAA = FJB+FJC+FMA+1. $ ICC = -FJA+FJB+FJC+1.
      IFF = FJA-FJB+FJC+1. $ IGG = G+1.
      J1M = B+1. $ J2M = P+1. $ J3M = D+1.
      J1P = FJA+FMA+1. $ J2P = FJB+FMB+1. $ J3P = FJC+FMC+1.
      E2 = GAM(J1M)*GAM(J1P)*GAM(J2M)*GAM(J2P)
      E1 = (GAM(ICC)*GAM(IFF)/GAM(IHH))*GAM(IGG)*GAM(J3M)*GAM(J3P)
      E1 = SQRT(E2/E1)
      E = FJA - FJB + FMC
      IAEE = ABS(E) + 0.001
      IEE = IAEE + 1  $  I1 = 0
      IF (E.GE.0.) GO TO 100
      IEE = -IAEE + 1  $  I1 = IAEE
  100 I2 = ICC - 1
      IF (J3M.LT.ICC) I2 = J3M - 1
      DO 150 I=I1,I2
      E2 = GAM(I+1)*GAM(ICC-I)*GAM(J3M-I)/GAM(IAA-I)
  150 S3J = S3J+(((-1.)**(I-(I/2)*2))/E2)*GAM(J1M+I)/GAM(IEE+I)
      I = ABS(FJA+FMB-FMC) + 0.01
      S3J = S3J * ((-1.)**(I-(I/2)*2))/E1
      RETURN
      END
C
C
      SUBROUTINE WEDDLE (DX, N, F, A, F0)
C
C     INTEGRATION SUBROUTINE
      DIMENSION F(N)
      A = 0.0  $  K = N - 1
      DO 15 I = 1,6
      SUM = 0.0
      DO 6 J = I, K, 6
    6 SUM = SUM + F(J)
      GO TO (8, 10, 12, 10, 8, 14), I
    8 A = A + 5.0 * SUM
      GO TO 15
   10 A = A + SUM
      GO TO 15
   12 A = A + 6.0 * SUM
```

```
      GO TO 15
   14 A = A + 2.0 * SUM
   15 CONTINUE
      A = 0.3 * DX * (A + F0 + F(N))
      RETURN
      END
C
C
      FUNCTION WFLD(B)
C
C     CALCULATION OF THE ION MICROFIELD DISTRIBUTION FUNCTION USING A
C     5POINT INTERPOLATION FOR THE DATA READ INTO THE MAINPROGRAM
      COMMON/PFW/FIELD(301)
      WFLD = 0.0
      IF (B.LE.30.0) GO TO 200
      SBS = 1./(B * SQRT(B))
      WFLD = ((21.6 * SBS + 7.639) * SBS + 1.496) * SBS/B
      RETURN
  200 IF (B.LE.0.0) RETURN
      J = (B + 0.2) * 10.0
      L = J - 1
      IF (J.GT.2) L = J - 2
      IF (J.GT.3) L = J - 3
      IF (J.GT.300) L = 297
   70 LLL = L + 4
      DO 75 K = L,LLL
      AK = K - 1
      TERM = 1.0
      DO 74 M = L,LLL
      IF (K.EQ.M) GO TO 74
      AM = M - 1
      TERM = TERM * (10.*B - AM)/(AK - AM)
   74 CONTINUE
      TERM = TERM * FIELD(K)
   75 WFLD = WFLD + TERM
      RETURN
      END
C
C
      FUNCTION COSINT(X)
C
C     CALCULATION OF THE COSINE INTEGRAL
      TYPE DOUBLE Y2,PROD,SUM,PT,DK
      IF(X.LE.0.) GO TO 50
      X2 = X * X
      IF(X.GT.20.) GO TO 30
      Y2 = DBLE(X2)  $  PROD = -Y2 * 0.5  $  SUM = PROD * 0.5
      DO 10 K = 2,50
      DK = 2 * K
      PROD = -PROD * Y2/(DK*(DK - 1.))
      SUM = SUM + PROD/DK
      PT = ABS(PROD * 1.D+10)
      IF(ABS(SUM).GT.PT) GO TO 20
   10 CONTINUE
   20 SS = SNGL(SUM)
      COSINT = SS  + 0.5772156649 + LOGF(X)
      RETURN
   30 FA = 1.  $  FB = 1.  $  P0 = 1.
      X2 = 1./X2
      DO 40 K = 1,10
      AK = 2 * K  $  P0 = -P0 * AK * X2  $  FA = FA + P0
      P0 = P0 * (AK + 1.)  $  FB = FB + P0  $  PA = ABS(P0 * 1.E+10)
      IF(PA.LE.FB) GO TO 45
```


406-848 O - 71 - 3

```
   40 CONTINUE
   45 FX = FA/X
      GX = FB * X2
      COSINT = FX * SIN(X) - GX * COS(X)
      RETURN
   50 WRITE (61,100) X
  100 FORMAT (* X LESS OR EQUAL TO ZERO, X = *E17.9)
      RETURN
      END
C
C
      SUBROUTINE BSJY01 (X, AJ0, Y0, AJ1, Y1)
C
C     CALCULATION OF THE BESSEL FUNCTIONS J0, Y0, J1, AND Y1 FOR AN
C     ARGUMENT X
      DIMENSION A(7), B(7), C(7), D(7), E(7), F(7), G(7), H(7)
      DATA ((A(I), I = 1,7) =  0.00021, -0.0039444, 0.0444479,
     1   -0.3163866, 1.2656208, -2.2499997, 1.0)
      DATA ((B(I), I = 1,7) = -0.00024846, 0.00427916, -0.04261214,
     1   0.25300117, -0.74350384, 0.60559366, 0.36746691)
      DATA ((C(I), I = 1,7) =  0.00014476, -0.00072805, 0.00137237,
     1   -0.00009512, -0.0055274, -0.00000077, 0.79788456)
      DATA ((D(I), I = 1,7) =  0.00013558, -0.00029333, -0.00054125,
     1   0.00262573, -0.00003954, -0.04166397, -0.78539816)
      DATA ((E(I), I = 1,7) =  0.00001109, -0.00031761, 0.00443319,
     1   -0.03954289, 0.21093573, -0.56249985, 0.5)
      DATA ((F(I), I = 1,7) =  0.0027873, -0.0400976, 0.3123951,
     1   -1.3164827, 2.1682709, 0.2212091, -0.6366198)
      DATA ((G(I), I = 1,7) = -0.00020033, 0.00113653, -0.00249511,
     1   0.00017105, 0.01659667, 0.00000156, 0.79788456)
      DATA ((H(I), I = 1,7) = -0.00029166, 0.00079824, 0.00074348,
     1   -0.00637879, 0.0000565, 0.12499612, -2.35619449)
      AX = ABSF(X)
      IF (AX.GT.0.0) GO TO 10
      AJ0 = 1.  $  Y0 = -1.E+30  $  AJ1 = 0.  $  Y1 = -1.E+30
      RETURN
 10   IF (AX.GT.3.0) GO TO 50
      XX = (AX/3.0) ** 2
      AJ0 = A(1)  $  Y0 = B(1)  $  AJ1 = E(1)  $  Y1 = F(1)
      DO 20 M = 2,7
      AJ0 = AJ0 * XX + A(M)
      Y0 = Y0 * XX + B(M)
      AJ1 = AJ1 * XX + E(M)
 20   Y1 = Y1 * XX + F(M)
      AJ1 = AJ1 * X
      ALF = 0.6366197724 * LOGF(0.5 * AX)
      Y0 = Y0 + ALF * AJ0
      Y1 = Y1/X + ALF * AJ1
      RETURN
 50   X3 = 3.0/AX
      F0 = C(1)  $  TH0 = D(1)  $  F1 = G(1)  $  TH1 = H(1)
      DO 60 M = 2,7
      F0 = F0 * X3 + C(M)
      TH0 = TH0 * X3 + D(M)
      F1 = F1 * X3 + G(M)
 60   TH1 = TH1 * X3 + H(M)
      TH0 = TH0 + AX  $  TH1 = TH1 + AX
      XS = 1./SQRT(AX)
      AJ0= XS * F0 * COSF(TH0)  $  Y0 = XS * F0 * SINF(TH0)
      AJ1= XS * F1 * COSF(TH1)  $  Y1 = XS * F1 * SINF(TH1)
      RETURN
      END
C
```

```
C
C
      PROGRAM STBRHY
C
C     PROGRAM FOR CALCULATING THE STARKBROADENING OF HYDROGEN ON THE
C     BASIS OF THE UNIFIED THEORY WITHOUT LOWER STATE INTERACTION
      DIMENSION DQQ(247),PFAC(6),STRONG(50),FF(1100),SJUU(136,31),
     1   SJLL(6,5),RDM(16,3),SLUU(16),SLLL(3),NST(50),DST(50),W(300,5),
     2   DIP(16,3,20),FPAR(6,50)
      COMMON/FDAT/P1,P2,B1,A2,B2,PPFF,CCREAL,CCIMAG
      COMMON/PFW/FIELD(301)
      COMMON/11/SLOP(16,16,60)
      COMMON/22/DIPOL(16,16,20),NSTEP,FPPP(6,15),NNUU,NNLL,BET
      COMMON/33/AMATR(34,68), BMATR(34,34), CMATR(34,34)
      EQUIVALENCE (SJUU,AMATR)
      FIELD(1) = 0.0
      READ 100, ((W(I,J), J = 1,5), I = 1,300)
  100 FORMAT (5E12.4)
  120 READ 150, DEN,TEMP,NNUU,NNLL,GIN,DGG,NTOT,NFAC,(PFAC(I),I=1,6)
  150 FORMAT (2E10.2,I3,I2,2F10.2,2I5/6F10.5)
      IF (EOF,60) 577, 170
C     CALCULATION OF MICROFIELD DISTRIBUTION FUNCTION
  170 SHIELD = 0.0898 * DEN**(1./6.)/SQRT(TEMP)
      DO 161 J = 1,5
  161 DST(J) = 0.2 * FLOAT(J-1)
      DO 163 I = 1,300
      DO 162 J = 1,5
  162 DQQ(J) = W(I,J)
      CALL POLY5 (DST,DQQ,5,STRONG,SLUU,SHIELD,0.1,1)
  163 FIELD(I+1) = SLUU(1)
C     CALCULATION OF AVERAGE IONFIELD
      DO 111 I = 1,300
      AM = I
  111 FF(I) = FIELD(I+1) * AM/10.
      CALL WEDDLE (0.1,300,FF,BAV,0.)
      DY = 1./300.  $  Y = 0.
      DO 113 I = 1,10
      Y = Y + DY  $  B = 1./Y
  113 FF(I) = WFLD(B) * B**3
      CALL WEDDLE (DY,10,FF,DB,0.)
      BAV = BAV + DB
C     CALCULATION OF WAVELENGTH IN STANDARD AIR
  178 AUU = NNUU
      ALL = NNLL
      SL1 = 109678.758 * (1./(ALL*ALL) - 1./(AUU*AUU))
      SL2 = SL1 * SL1
      ALDD = 1.000064328+2949810./(1.46E+10-SL2)+25540./(4.1E+9-SL2)
      ALAM = 1.E+8/(ALDD * SL1)
      PRINT 180, DEN, TEMP, NNUU, NNLL, ALAM, SHIELD
  180 FORMAT (1H1,*  DENSITY =* E10.2* TEMPERATURE =*E10.2,
     1   * QUANTUMNUMBERS  N UPPER =*I3*  N LOWER =*I2* WAVELENGTH =*
     2   F8.2* ANGSTROM*/10X,*SHIELDING PARAMETER =*F6.3,10X,
     3   * NO LOWER STATE INTERACTION *//)
      IF (NNUU.LE.16.AND.NNLL.LE.3) GO TO 200
      PRINT 190
  190 FORMAT (* OVERFLOW OF MATRICES, PROGRAM NOT EXECUTED*)
  577 CALL EXIT
C
C     RADIAL MATRIXELEMENTS AND TOTAL LINESTRENGTH
  200 IPI = MOD(NNUU-NNLL,2) + 1
      STOT = 0.
      DO 330 KLL = 1,NNLL
      LLL = KLL - 1  $  ALL = LLL
```

```
      DO 310 KUU = 1,NNUU
      LUU = KUU - 1  $  AUU = LUU  $  RRMM = 0.
      IF (IABS(KUU - KLL).NE.1) GO TO 310
      RRMM = RADMAT(NNUU,LUU,NNLL,LLL) * S3J(ALL,AUU,1.,0.,0.,0.)
      STOT = STOT + (2.*ALL+1.)*(2.*AUU+1.) * RRMM * RRMM
 310  RDM(KUU,KLL) = RRMM
 330  CONTINUE
      SQST = SQRT(STOT)
C
C     TRANSFORMATION MATRICES
      DO 370 NKK = 1,2
      NN = NNLL
      IF (NKK.EQ.2) NN = NNUU
      ANN = NN  $  AN1 = 0.5 * (ANN - 1.)
      KQQ = 2 * NN - 1  $  NRUN = 0
      DO 370 KL = 1,NN
      AL = KL - 1
      FACC = SQRT(2.*AL+1.)
      IF(NKK.EQ.1) SLLL(KL) = FACC
      IF(NKK.EQ.2) SLUU(KL) = FACC
      DO 370 KM = 1,KL
      AM = KM - 1  $  NRUN = NRUN + 1
      QQ = -ANN  $  ALIM = ANN - 0.9 - AM
      DO 370 KQ = 1,KQQ
      QQ = QQ + 1.  $  SIIJ = 0.  $  ABQQ = ABS(QQ)
      IF (ABQQ.GT.ALIM) GO TO 360
      NQ = ABQQ + 0.1
      IF (MOD(NN+NQ+KM+1,2).NE.1) GO TO 360
      AMQ = 0.5 * (AM - QQ)  $  APQ = 0.5 * (AM + QQ)
      SIIJ = FACC * S3J(AN1,AN1,AL,AMQ,APQ,-AM)
 360  IF (NKK.EQ.1) SJLL(NRUN,KQ) = SIIJ
      IF (NKK.EQ.2) SJUU(NRUN,KQ) = SIIJ
 370  CONTINUE
C
C     DIPOLMATRIXELEMENTS IN PARABOLIC STATES
      NQMAX = NNUU * (NNUU-1) + NNLL * (NNLL-1) + 1
      DO 490 MM = 1,NQMAX
 490  DQQ(MM) = 0.
      MMAX = NNLL + 1  $  KQLL = 2 * NNLL - 1
      DO 500 MM = 1,MMAX
      MMU = MM - 1  $  AMU = MMU  $  AMLCK = 1.
      IF (MM.GT.1) AMLCK = 2.
      NAQU = -NNUU + MMU - 1  $  KQUU = NNUU - MMU
      DO 500 KUU = 1,KQUU
      NAQU = NAQU + 2  $  KQU = NNUU + NAQU  $  NAQL = -NNLL
      DO 500 KLL = 1,KQLL
      NRUN = MMU * KQLL + KLL  $  NAQL = NAQL + 1  $  KQL = NNLL + NAQL
      NXDIF = NNUU * NAQU - NNLL * NAQL + 1
      MML = MMU - 2  $  KMINL = NNLL - IABS(NAQL) - 1
      DO 470 KAML = 1,3
      SIIJ = 0.  $  MML = MML + 1
      IF (MOD(NNLL+NAQL+MML,2).NE.1) GO TO 470
      IF (IABS(MML).GT.KMINL) GO TO 470
      AML = MML  $  AMBL = AMU - AML
      NPHAS = (NNUU + MMU - NAQU + NNLL - MML - NAQL - 2)/2
      PHASE = (-1.)**MOD(NPHAS,2)
      RESULT = 0.  $  KBBU = IABS(MMU) + 1  $  KBBL = IABS(MML) + 1
      DO 450 KKLU = KBBU,NNUU
      ALU = KKLU - 1
      LLU = (KKLU-1) * KKLU / 2 + KBBU
      FAC1 = SLUU(KKLU) * SJUU(LLU,KQU)
      DO 450 KKLL = KBBL,NNLL
      IF (IABS(KKLU - KKLL).NE.1) GO TO 450
```

```
      ALL = KKLL - 1
      LLL = (KKLL - 1) * KKLL / 2 + KBBL
      FAC2 = SLLL(KKLL) * SJLL(LLL,KQL)
      FACC = FAC2 * FAC1 * S3J(ALL,ALU,1.,AML,-AMU,AMBL)
      RESULT = RESULT + FACC * RDM(KKLU,KKLL)
  450 CONTINUE
      SIIJ = RESULT * PHASE / SQST
      PRINT 425,NAQU,MMU,NAQL,MML,SIIJ
  425 FORMAT (16X,*(*,2I3,*  I D I*,2I3,* )  =*E16.8)
      IF (NXDIF.GT.0) DQQ(NXDIF) = DQQ(NXDIF) + AMLCK*RESULT*RESULT/STOT
  470 DIP(KUU,KAML,NRUN) = SIIJ
  500 CONTINUE
      PRINT 393
  393 FORMAT(/)
      DO 440 MM= 1,MMAX
      MMU = MM - 1  $  KQUU = NNUU - MMU  $  AMLCK = 1.
      IF (MMU.GT.0) AMLCK = 2.
      DO 440 KLL = 1,KQLL
      NRUN = MMU * KQLL + KLL
      DO 440 NRA = 1,KQUU
      DO 440 NRB = 1,KQUU
      SIIJ = 0.
      DO 420 KAML = 1,3
  420 SIIJ = SIIJ + AMLCK*DIP(NRA,KAML,NRUN)*DIP(NRB,KAML,NRUN)
  440 DIPOL(NRA,NRB,NRUN) = SIIJ
      DST(1) = DQQ(1)  $  NST(1) = 0  $  KMST = IPI - 1
      DO 430 NXDIF = 2,NQMAX
      IF (DQQ(NXDIF).LT.1.E-20) GO TO 430
      KMST = KMST + 1  $  DST(KMST) = DQQ(NXDIF)  $ NST(KMST) = NXDIF-1
  430 CONTINUE
      PRINT 355, (NST(I),DST(I),I = 1,KMST)
  355 FORMAT (16X,*X =*I3,F20.10)
      PRINT 393
C
C     K OPERATOR MATRIX
      NTIME = KLOCK(0)  $  NCM1 = NNUU - 1
      DO 600 MM = 1,MMAX
      MMU = MM - 1  $  AMU = MMU
      DO 600 NRC = 1,NCM1
      NRUN = MMU * NCM1 + NRC  $  KCQU = NNUU + NRC
      NAQU = -NNUU + MMU - 1  $  KQUU = NNUU - MMU
      DO 600 NRA = 1,KQUU
      NAQU = NAQU + 2  $  KAQU = NNUU + NAQU  $ NBQU = -NNUU + MMU - 1
      DO 600 NRB = 1,NRA
      NBQU = NBQU + 2  $  KBQU = NNUU + NBQU  $  SIIJ = 0.
      DO 540 JLAU = MM,NNUU
      ALU = JLAU - 1
      LALU = (JLAU-1)*JLAU/2 + MM
      FAC1 = SJUU(LALU,KAQU) * SJUU(LALU,KBQU)
      FAC2 = 0.  $  KMINL = MINO(JLAU,NNUU-NRC)
      DO 520 JMCU = 1,KMINL
      IF (MOD(NNUU+NRC+JMCU,2).EQ.1) GO TO 520
      LCLU = LALU - MM + JMCU  $  AMC = 1.
      IF (JMCU.GT.1) AMC = 2.
      NPHAS = MM + JMCU + NRC - (NAQU+NBQU)/2
      PHASE = (-1.)**MOD(NPHAS,2)
      FAC2 = FAC2 + PHASE*AMC*(SJUU(LCLU,KCQU))**2
  520 CONTINUE
  540 SIIJ = SIIJ + FAC1 * FAC2/(2.*ALU+1.)
      SLOP(NRA,NRB,NRUN) = SIIJ
  600 SLOP(NRB,NRA,NRUN) = SIIJ
      NTIME = -NTIME + KLOCK(0)
      PRINT 617, NTIME
```

```
 617  FORMAT (16X,*COMPUTERTIME FOR CALCULATING K-OPERATOR MATRIX =*I8/)
C
C      BASIC CONSTANTS AND ARRAY FOR G-FUNCTION CONSTANTS
       SDEN = SQRT(DEN)
       FAC = 2064.936 * TEMP * SQRT(TEMP/DEN)
       CFAC = 4.5645E-7 * SDEN/TEMP
       DEBROG = 2.1027E-6/SQRT(TEMP)
       ANN = NNUU
       RMIN = DEBROG + ANN * ANN * 7.9376E-9
       BET = 5.6558E-5 * DEN**(1./6.)
       ASY = 0.0
       DO 270 NRC = IPI,KMST
       QC = NST(NRC)  $  C = CFAC * QC
       P1 = -1.671086 * FAC * C * SQRT(C)
       BS = 3. * QC * DEBROG / RMIN
       STRONG(NRC) = 0.269-2.*(((1.-COSF(BS))/BS+SINF(BS))/BS-COSINT(BS))
       PPFF = -1.128379 * FAC * C * C
       P2 = PPFF * (STRONG(NRC)-2.*LOGF(2.*C))
       FPAR(1,NRC) = P1  $  FPAR(2,NRC) = P2
       FPAR(3,NRC) = 0.5 * (P2/P1)**2  $  FIN = LOGF(QC)
       A2 = P2*((PFAC(3)*FIN+PFAC(2))*FIN+PFAC(1))
       B2 = (PFAC(6)*FIN+PFAC(5))*FIN + PFAC(4)
       IF (B2.LT.0.) A2 = 0.
       FPAR(4,NRC) = A2  $  FPAR(5,NRC) = B2  $ FPAR(6,NRC) = PPFF
 270   ASY = ASY + 2. * P1 * DST(NRC)
       DO 275 NRC = 1,NCM1
       NCC = NRC * NNUU
       DO 278 NRA = IPI,KMST
       IF(NST(NRA).EQ.NCC) GO TO 279
 278   CONTINUE
 279   FPPP(1,NRC) = FPAR(1,NRA)  $  FPPP(2,NRC) = FPAR(2,NRA)
       FPPP(3,NRC) = FPAR(3,NRA)  $  FPPP(4,NRC) = FPAR(4,NRA)
       FPPP(5,NRC) = FPAR(5,NRA)
 275   FPPP(6,NRC) = FPAR(6,NRA)
       PRINT 220
 220   FORMAT (/13X*P1*18X*P2*18X*B1*18X*A2*18X*B2*17X*STRONG*/)
       PRINT 240,((FPAR(K,I),K = 1,5),STRONG(I), I = IPI,KMST)
 240   FORMAT (6E20.4)
       PRINT 280, FAC, CFAC, BET, ASY, DEBROG, BAV, NFAC
 280   FORMAT(/* FAC =*E11.4,* CFAC =*E11.4,* BET =*E11.4,* ASY =*E11.4,
      1    * DEBROG =*E11.4,* BAV =*F7.4,* INTEGRATIONFACTOR =*I2//
      2    5X*DOM*8X*DLAM*8X*ITOT*6X*IHOLTS*8X*ASY*10X*WING*7X*WHOLTS*7X,
      3    *WW00*8X*WWBB*8X*WWNG*8X*TIME  STEPS*/)
       ADLFAC = 4.23538E-15 * SDEN * ALAM * ALAM
C
C      CALCULATION OF THE IONFIELD INTEGRAL
       N12 = 12 * NFAC  $  AN12 = N12  $  N30 = 30 * NFAC  $  AN30 = N30
       DMCRT = BET * BAV * NST(KMST) * 5.
       G = GIN - DGG
       DO 950 MM = 1,NTOT
       NTIME = KLOCK(0)
       NSTEP = 0  $  G = G + DGG
       DOM = 10. ** G  $  DLAM = ADLFAC * DOM
       WING52 = -0.2992067103 * ASY/(SQRT(DOM) * DOM * DOM)
       FHOLTS = 0.  $  AWING = 0.
       DO 815 NRC = IPI,KMST
       P1 = FPAR(1,NRC)  $  P2 = FPAR(2,NRC)  $  B1 = FPAR(3,NRC)
       A2 = FPAR(4,NRC)  $  B2 = FPAR(5,NRC)  $  PPFF = FPAR(6,NRC)
       CALL FOUTR(DOM)
       AWING = AWING + DST(NRC) * CCIMAG * 2./(DOM*DOM)
       QC = NST(NRC)  $  BETFAC = BET * QC  $  BCRIT = DOM/BETFAC
 815   FHOLTS = FHOLTS + DST(NRC) * WFLD(BCRIT) / BETFAC
       IF (DOM.GT.DMCRT) GO TO 985
```

```
      AIRES = 0.
      IF(DOM.GT.(-3.*P2)) GO TO 840
      ANQ1 = NST(KMST)
      BCRIT = (DOM - P2)/(ANQ1*BET)
      DB = BCRIT/AN12  $  B = 0.
      DO 820 J = 1,N12
      B = B + DB
  820 FF(J) = AIIM(DOM,B) * WFLD(B)
      CALL WEDDLE (DB,N12,FF,AIII,0.)
      AIRES = AIII
      DY = 1./(BCRIT*AN30)  $  Y = 0.
      DO 830 J = 1,N30
      Y = Y + DY  $  B = 1./Y
  830 FF(J) = B * B * AIIM(DOM,B) * WFLD(B)
      CALL WEDDLE (DY,N30,FF,AIII,0.)
      AIRES = AIRES + AIII
      GO TO 980
  840 BCRCR = DOM/BET
      EPSPS = -P2/BET
      DO 957 NQ = IPI,KMST
      ANQ = NST(NQ)
      BCR = BCRCR/ANQ  $  EPS = EPSPS/ANQ
      IF (NQ.EQ.IPI) GO TO 907
      SL1 = 1./(GAM - BCR)
      GO TO 908
  907 SL1 = 0.
  908 SL2 = 1./EPS
      SL3 = 1./(BCR + EPS)  $  SL4 = 1./(BCR - EPS)
      IF (NQ.EQ.KMST) GO TO 911
      ANQ1 = NST(NQ+1)
      GAM = 0.5 * (BCR-EPS+(BCRCR+EPSPS)/ANQ1)
      GO TO 912
  911 GAM = 0.5 * (BCR-EPS)
  912 SL5 = 1./(BCR-GAM)
      CRIT = SL2 - SL5
  904 Y = SL1
      IF (NQ.EQ.IPI) GO TO 913
      B = BCR + 1./Y
      FA = AIIM(DOM,B) * WFLD(B)/(Y * Y)
      GO TO 914
  913 FA = 0.
  914 DY = (SL2 - SL1)/AN12
      DO 917 J = 1,N12
      Y = Y + DY  $  Y1 = 1./Y  $  B = BCR + Y1
  917 FF(J) = Y1 * Y1 * AIIM(DOM,B) * WFLD(B)
      CALL WEDDLE (DY,N12,FF,AIII,FA)
      AIRES = AIRES + AIII
      Y = SL3  $  B = 1./Y
      FA = B * B * AIIM(DOM,B) * WFLD(B)
      DY = (SL4 - SL3)/AN12
      DO 927 J = 1,N12
      Y = Y + DY  $  B = 1./Y
  927 FF(J) = B * B * AIIM(DOM,B) * WFLD(B)
      CALL WEDDLE (DY,N12,FF,AIII,FA)
      AIRES = AIRES + AIII
      IF(CRIT.LE.0.) GO TO 977
      Y = SL5  $  B = BCR - 1./Y
      FA = AIIM(DOM,B) * WFLD(B)/(Y * Y)
      DY = CRIT/AN12
      DO 937 J = 1,N12
      Y = Y + DY  $  Y1 = 1./Y  $  B = BCR - Y1
  937 FF(J) = Y1 * Y1 * AIIM(DOM,B) * WFLD(B)
      CALL WEDDLE (DY,N12,FF,AIII,FA)
```

```
      AIRES = AIRES + AIII
  957 CONTINUE
      IF(GAM.LT. 5.) GO TO 968
      Y = 1./GAM  $  DY = (0.2 - Y)/AN12
      FA = GAM * GAM * AIIM(DOM,GAM) * WFLD(GAM)
      DO 967 J = 1,N12
      Y = Y + DY  $  B = 1./Y
  967 FF(J) = B * B * AIIM(DOM,B) * WFLD(B)
      CALL WEDDLE (DY,N12,FF,AIII,FA)
      AIRES = AIRES + AIII
      SL4 = 0.2
      GO TO 977
  968 SL4 = 1./GAM
  977 B = 0.
      DB = 1./(SL4 * AN30)
      DO 947 J = 1,N30
      B = B + DB
  947 FF(J) = AIIM(DOM,B) * WFLD(B)
      CALL WEDDLE (DB,N30,FF,AIII,0.)
      AIRES = AIRES + AIII
  980 WWBB = (AIIM(DOM,BAV) + FHOLTS)/WING52
      GO TO 990
  985 AIRES = AIIM(DOM,BAV) + FHOLTS
      WWBB = 0.
  990 WING = AIRES/WING52
      WINHOL = FHOLTS/WING52
      WW00 = (AIIM(DOM, 0.) + FHOLTS)/WING52
      WWNG = (AWING + FHOLTS)/WING52
      NTIME = -NTIME + KLOCK(0)
  950 PRINT 978,DOM,DLAM,AIRES,FHOLTS,WING52,WING,WINHOL,WW00,WWBB,
     1   WWNG,NTIME,NSTEP
  978 FORMAT (10E12.4,I10,I6)
      GO TO 120
      END
C
C
      FUNCTION AIIM(DOM,B)
C
C     CALCULATION OF I(DOM,B) FOR THE CASE OF NO LOWER STATE INTERACTION
      DIMENSION DRRF(15), DIIF(15), FMATR(15,15)
      COMMON/FDAT/P1,P2,B1,A2,B2,PPFF,CCREAL,CCIMAG
      COMMON/11/SLOP(16,16,60)
      COMMON/22/DIPOL(16,16,20),NSTEP,FPPP(6,15),NNUU,NNLL,BET
      COMMON/33/AMATR(34,68), BMATR(34,34), CMATR(34,34)
      AIIM = 0.  $  NSTEP = NSTEP + 1
      MMAX = NNLL + 1  $  KQLL = 2 * NNLL - 1  $  NCM1 = NNUU - 1
      DO 800 MM = 1,MMAX
      MMU = MM - 1  $  NUPP = NNUU - MMU  $  NQL = -NNLL
      DO 800 KLL = 1,KQLL
      NQL = NQL + 1
      NRUN = MMU * KQLL + KLL  $  NBQU = -NNUU + MMU - 1
      DO 750 NRB = 1,NUPP
      NBQU = NBQU + 2  $  AXDIF = NNUU * NBQU - NNLL * NQL
      DOMRB = DOM - BET * B * AXDIF
      DO 220 NRC = 1,NCM1
      P1 = FPPP(1,NRC)  $  P2 = FPPP(2,NRC)  $  B1 = FPPP(3,NRC)
      A2 = FPPP(4,NRC)  $  B2 = FPPP(5,NRC)  $  PPFF = FPPP(6,NRC)
      CALL FOUTR(DOMRB)
      DRRF(NRC) = CCREAL
  220 DIIF(NRC) = CCIMAG
      DO 700 NRA = 1,NUPP
      ARRR = 0.  $  AIII = 0.
      DO 600 NRC = 1,NCM1
```

```
      MQC = MMU * NCM1 + NRC
      TEMP = SLOP(NRB,NRA,MQC)
      ARRR = ARRR + TEMP * DRRF(NRC)
  600 AIII = AIII + TEMP * DIIF(NRC)
      AIII = AIII * 6.2831853072
      AMATR(NRB,NRA) = AIII  $  CMATR(NRB,NRA) = AIII
  700 BMATR(NRB,NRA) = ARRR * 6.2831853072
  750 BMATR(NRB,NRB) = BMATR(NRB,NRB) + DOMRB
      CALL ENVERS (NUPP)
      DO 320 NRB = 1,NUPP
      DO 320 NRA = 1,NUPP
      TEMP = 0.
      DO 300 NRC = 1,NUPP
  300 TEMP = TEMP + BMATR(NRB,NRC) * AMATR(NRC,NRA+NUPP)
  320 FMATR(NRB,NRA) = TEMP
      DO 420 NRB = 1,NUPP
      DO 420 NRA = 1,NUPP
      TEMP = 0.
      DO 400 NRC = 1,NUPP
  400 TEMP = TEMP + FMATR(NRB,NRC) * BMATR(NRC,NRA)
  420 AMATR(NRB,NRA) = TEMP + CMATR(NRB,NRA)
      CALL ENVERS (NUPP)
      DO 795 NRB = 1,NUPP
      DO 795 NRA = 1,NUPP
  795 AIIM = AIIM + DIPOL(NRB,NRA,NRUN)*AMATR(NRB,NRA+NUPP)
  800 CONTINUE
      AIIM =  AIIM * 0.3183099  $  RETURN
      END
C
C
```

LOW FREQUENCY COMPONENT OF THE ELECTRIC MICROFIELDS

$r_0/D=0$	=0.2	=0.4	=0.6	=0.8	10β
4.2200−003	6.9547−003	1.1584−002	1.9378−002	3.3258−002	1
1.6670−002	2.7217−002	4.4735−002	7.3201−002	1.2093−001	2
3.6640−002	5.9060−002	9.5010−002	1.5018−001	2.3439−001	3
6.3080−002	9.9852−002	1.5606−001	2.3598−001	3.4416−001	4
9.4600−002	1.4638−001	2.2090−001	3.1741−001	4.3106−001	5
1.2959−001	1.9523−001	2.8304−001	3.8512−001	4.8799−001	6
1.6636−001	2.4312−001	3.3742−001	4.3436−001	5.1632−001	7
2.0323−001	2.8721−001	3.8073−001	4.6430−001	5.2143−001	8
2.3864−001	3.2532−001	4.1151−001	4.7674−001	5.0966−001	9
2.7122−001	3.5597−001	4.2978−001	4.7485−001	4.8675−001	10
2.9987−001	3.7845−001	4.3663−001	4.6214−001	4.5729−001	11
3.2378−001	3.9268−001	4.3381−001	4.4193−001	4.2466−001	12
3.4246−001	3.9910−001	4.2331−001	4.1702−001	3.9118−001	13
3.5570−001	3.9855−001	4.0710−001	3.8961−001	3.5839−001	14
3.6357−001	3.9206−001	3.8700−001	3.6133−001	3.2718−001	15
3.6633−001	3.8077−001	3.6450−001	3.3333−001	2.9807−001	16
3.6445−001	3.6584−001	3.4084−001	3.0635−001	2.7128−001	17
3.5850−001	3.4831−001	3.1694−001	2.8086−001	2.4685−001	18
3.4911−001	3.2911−001	2.9347−001	2.5712−001	2.2470−001	19
3.3694−001	3.0904−001	2.7090−001	2.3522−001	2.0473−001	20
3.2265−001	2.8872−001	2.4953−001	2.1516−001	1.8675−001	21
3.0684−001	2.6865−001	2.2952−001	1.9689−001	1.7058−001	22
2.9005−001	2.4918−001	2.1096−001	1.8031−001	1.5607−001	23
2.7275−001	2.3058−001	1.9385−001	1.6529−001	1.4303−001	24
2.5537−001	2.1300−001	1.7816−001	1.5170−001	1.3131−001	25

LOW FREQUENCY COMPONENT OF THE ELECTRIC MICROFIELDS

$r_0/D=0$	$=0.2$	$=0.4$	$=0.6$	$=0.8$	10β
2.3822−001	1.9654−001	1.6382−001	1.3942−001	1.2077−001	26
2.2156−001	1.8124−001	1.5075−001	1.2832−001	1.1129−001	27
2.0557−001	1.6709−001	1.3885−001	1.1829−001	1.0273−001	28
1.9037−001	1.5406−001	1.2804−001	1.0922−001	9.5010−002	29
1.7606−001	1.4211−001	1.1821−001	1.0100−001	8.8028−002	30
1.6268−001	1.3116−001	1.0928−001	9.3560−002	8.1696−002	31
1.5024−001	1.2117−001	1.0117−001	8.6805−002	7.5951−002	32
1.3873−001	1.1204−001	9.3793−002	8.0667−002	7.0731−002	33
1.2812−001	1.0371−001	8.7081−002	7.5082−002	6.5969−002	34
1.1837−001	9.6123−002	8.0967−002	6.9993−002	6.1626−002	35
1.0942−001	8.9201−002	7.5392−002	6.5348−002	5.7662−002	36
1.0124−001	8.2886−002	7.0303−002	6.1103−002	5.4030−002	37
9.3751−002	7.7122−002	6.5651−002	5.7216−002	5.0700−002	38
8.6913−002	7.1857−002	6.1393−002	5.3652−002	4.7650−002	39
8.0670−002	6.7044−002	5.7491−002	5.0378−002	4.4839−002	40
7.4969−002	6.2639−002	5.3910−002	4.7366−002	4.2246−002	41
6.9762−002	5.8603−002	5.0620−002	4.4592−002	3.9859−002	42
6.5004−002	5.4901−002	4.7591−002	4.2033−002	3.7647−002	43
6.0652−002	5.1502−002	4.4801−002	3.9668−002	3.5594−002	44
5.6670−002	4.8376−002	4.2226−002	3.7480−002	3.3696−002	45
5.3023−002	4.5498−002	3.9847−002	3.5454−002	3.1932−002	46
4.9678−002	4.2844−002	3.7647−002	3.3574−002	3.0289−002	47
4.6606−002	4.0395−002	3.5608−002	3.1828−002	2.8766−002	48
4.3781−002	3.8130−002	3.3716−002	3.0204−002	2.7348−002	49
4.1180−002	3.6034−002	3.1959−002	2.8692−002	2.6021−002	50
3.8783−002	3.4092−002	3.0325−002	2.7282−002	2.4785−002	51
3.6571−002	3.2289−002	2.8803−002	2.5965−002	2.3631−002	52
3.4529−002	3.0613−002	2.7383−002	2.4734−002	2.2543−002	53
3.2640−002	2.9054−002	2.6058−002	2.3582−002	2.1527−002	54
3.0890−002	2.7601−002	2.4819−002	2.2502−002	2.0578−002	55
2.9266−002	2.6247−002	2.3659−002	2.1489−002	1.9681−002	56
2.7756−002	2.4981−002	2.2573−002	2.0538−002	1.8839−002	57
2.6347−002	2.3798−002	2.1554−002	1.9644−002	1.8052−002	58
2.5030−002	2.2690−002	2.0597−002	1.8803−002	1.7302−002	59
2.3800−002	2.1652−002	1.9697−002	1.8012−002	1.6593−002	60
2.2655−002	2.0678−002	1.8850−002	1.7266−002	1.5928−002	61
2.1588−002	1.9764−002	1.8053−002	1.6562−002	1.5294−002	62
2.0592−002	1.8904−002	1.7302−002	1.5898−002	1.4693−002	63
1.9662−002	1.8095−002	1.6593−002	1.5270−002	1.4129−002	64
1.8790−002	1.7332−002	1.5923−002	1.4676−002	1.3592−002	65
1.7969−002	1.6614−002	1.5290−002	1.4113−002	1.3079−002	66
1.7197−002	1.5935−002	1.4692−002	1.3580−002	1.2599−002	67
1.6470−002	1.5295−002	1.4125−002	1.3074−002	1.2142−002	68
1.5786−002	1.4689−002	1.3588−002	1.2594−002	1.1704−002	69
1.5140−002	1.4116−002	1.3079−002	1.2137−002	1.1294−002	70
1.4531−002	1.3573−002	1.2596−002	1.1703−002	1.0903−002	71
1.3956−002	1.3059−002	1.2138−002	1.1290−002	1.0525−002	72
1.3413−002	1.2571−002	1.1702−002	1.0897−002	1.0168−002	73
1.2898−002	1.2108−002	1.1288−002	1.0523−002	9.8296−003	74
1.2410−002	1.1669−002	1.0894−002	1.0167−002	9.5003−003	75
1.1947−002	1.1251−002	1.0519−002	9.8275−003	9.1900−003	76
1.1508−002	1.0854−002	1.0161−002	9.5035−003	8.8965−003	77
1.1092−002	1.0477−002	9.8208−003	9.1941−003	8.6096−003	78
1.0696−002	1.0117−002	9.4959−003	8.8986−003	8.3371−003	79
1.0320−002	9.7745−003	9.1858−003	8.6162−003	8.0805−003	80

LOW FREQUENCY COMPONENT OF THE ELECTRIC MICROFIELDS

$r_0/D=0$	$=0.2$	$=0.4$	$=0.6$	$=0.8$	10β
9.9640−003	9.4481−003	8.8896−003	8.3461−003	7.8286−003	81
9.6250−003	9.1370−003	8.6066−003	8.0876−003	7.5880−003	82
9.3020−003	8.8401−003	8.3360−003	7.8402−003	7.3633−003	83
8.9940−003	8.5568−003	8.0772−003	7.6032−003	7.1431−003	84
8.7000−003	8.2863−003	7.8295−003	7.3763−003	6.9313−003	85
8.4180−003	8.0279−003	7.5925−003	7.1588−003	6.7349−003	86
8.1490−003	7.7809−003	7.3654−003	6.9504−003	6.5428−003	87
7.8920−003	7.5447−003	7.1480−003	6.7505−003	6.3557−003	88
7.6450−003	7.3188−003	6.9395−003	6.5589−003	6.1826−003	89
7.4100−003	7.1025−003	6.7397−003	6.3749−003	6.0139−003	90
7.1850−003	6.8955−003	6.5481−003	6.1982−003	5.8473−003	91
6.9700−003	6.6971−003	6.3641−003	6.0284−003	5.6932−003	92
6.7640−003	6.5070−003	6.1876−003	5.8652−003	5.5444−003	93
6.5680−003	6.3246−003	6.0179−003	5.7081−003	5.3958−003	94
6.3800−003	6.1496−003	5.8548−003	5.5569−003	5.2582−003	95
6.2000−003	5.9814−003	5.6979−003	5.4113−003	5.1267−003	96
6.0270−003	5.8199−003	5.5469−003	5.2708−003	4.9939−003	97
5.8600−003	5.6645−003	5.4014−003	5.1353−003	4.8699−003	98
5.6980−003	5.5149−003	5.2611−003	5.0046−003	4.7530−003	99
5.5400−003	5.3709−003	5.1258−003	4.8783−003	4.6335−003	100
5.4133−003	5.2320−003	4.9952−003	4.7563−003	4.5206−003	101
5.2692−003	5.0980−003	4.8690−003	4.6382−003	4.4154−003	102
5.1306−003	4.9686−003	4.7470−003	4.5240−003	4.3074−003	103
4.9970−003	4.8435−003	4.6290−003	4.4133−003	4.2035−003	104
4.8682−003	4.7227−003	4.5148−003	4.3062−003	4.1081−003	105
4.7441−003	4.6057−003	4.4043−003	4.2024−003	4.0101−003	106
4.6244−003	4.4925−003	4.2973−003	4.1017−003	3.9140−003	107
4.5090−003	4.3828−003	4.1936−003	4.0042−003	3.8269−003	108
4.3976−003	4.2765−003	4.0932−003	3.9097−003	3.7380−003	109
4.2900−003	4.1736−003	3.9960−003	3.8181−003	3.6490−003	110
4.1861−003	4.0737−003	3.9018−003	3.7294−003	3.5690−003	111
4.0857−003	3.9770−003	3.8106−003	3.6435−003	3.4886−003	112
3.9887−003	3.8832−003	3.7224−003	3.5603−003	3.4065−003	113
3.8948−003	3.7923−003	3.6370−003	3.4800−003	3.3331−003	114
3.8041−003	3.7041−003	3.5545−003	3.4024−003	3.2610−003	115
3.7164−003	3.6188−003	3.4747−003	3.3274−003	3.1860−003	116
3.6314−003	3.5361−003	3.3977−003	3.2551−003	3.1188−003	117
3.5492−003	3.4560−003	3.3233−003	3.1854−003	3.0549−003	118
3.4696−003	3.3785−003	3.2515−003	3.1182−003	2.9870−003	119
3.3925−003	3.3034−003	3.1822−003	3.0534−003	2.9259−003	120
3.3177−003	3.2307−003	3.1153−003	2.9911−003	2.8694−003	121
3.2453−003	3.1603−003	3.0507−003	2.9309−003	2.8086−003	122
3.1751−003	3.0922−003	2.9883−003	2.8728−003	2.7527−003	123
3.1070−003	3.0262−003	2.9279−003	2.8167−003	2.7027−003	124
3.0410−003	2.9623−003	2.8694−003	2.7623−003	2.6481−003	125
2.9769−003	2.9003−003	2.8127−003	2.7096−003	2.5961−003	126
2.9147−003	2.8402−003	2.7576−003	2.6583−003	2.5509−003	127
2.8543−003	2.7819−003	2.7040−003	2.6083−003	2.5013−003	128
2.7957−003	2.7253−003	2.6519−003	2.5594−003	2.4521−003	129
2.7387−003	2.6702−003	2.6009−003	2.5116−003	2.4100−003	130
2.6834−003	2.6167−003	2.5512−003	2.4646−003	2.3643−003	131
2.6296−003	2.5647−003	2.5025−003	2.4185−003	2.3170−003	132
2.5774−003	2.5141−003	2.4549−003	2.3732−003	2.2769−003	133
2.5266−003	2.4648−003	2.4082−003	2.3286−003	2.2346−003	134
2.4772−003	2.4169−003	2.3625−003	2.2848−003	2.1890−003	135

LOW FREQUENCY COMPONENT OF THE ELECTRIC MICROFIELDS

$r_0/D=0$	$=0.2$	$=0.4$	$=0.6$	$=0.8$	10β
2.4291−003	2.3703−003	2.3178−003	2.2417−003	2.1505−003	136
2.3824−003	2.3249−003	2.2740−003	2.1994−003	2.1115−003	137
2.3369−003	2.2807−003	2.2311−003	2.1578−003	2.0682−003	138
2.2926−003	2.2378−003	2.1892−003	2.1171−003	2.0313−003	139
2.2495−003	2.1961−003	2.1482−003	2.0773−003	1.9960−003	140
2.2075−003	2.1555−003	2.1083−003	2.0384−003	1.9555−003	141
2.1667−003	2.1162−003	2.0694−003	2.0004−003	1.9205−003	142
2.1268−003	2.0779−003	2.0314−003	1.9634−003	1.8890−003	143
2.0880−003	2.0408−003	1.9945−003	1.9274−003	1.8519−003	144
2.0502−003	2.0048−003	1.9587−003	1.8924−003	1.8189−003	145
2.0134−003	1.9698−003	1.9238−003	1.8585−003	1.7909−003	146
1.9775−003	1.9358−003	1.8899−003	1.8255−003	1.7575−003	147
1.9424−003	1.9029−003	1.8571−003	1.7935−003	1.7264−003	148
1.9083−003	1.8708−003	1.8251−003	1.7625−003	1.7015−003	149
1.8750−003	1.8397−003	1.7941−003	1.7325−003	1.6717−003	150
1.8425−003	1.8094−003	1.7640−003	1.7033−003	1.6424−003	151
1.8108−003	1.7799−003	1.7347−003	1.6751−003	1.6199−003	152
1.7798−003	1.7511−003	1.7062−003	1.6476−003	1.5936−003	153
1.7496−003	1.7230−003	1.6785−003	1.6209−003	1.5657−003	154
1.7201−003	1.6955−003	1.6515−003	1.5951−003	1.5449−003	155
1.6913−003	1.6687−003	1.6252−003	1.5699−003	1.5216−003	156
1.6632−003	1.6424−003	1.5995−003	1.5453−003	1.4949−003	157
1.6357−003	1.6166−003	1.5744−003	1.5214−003	1.4750−003	158
1.6089−003	1.5913−003	1.5498−003	1.4981−003	1.4541−003	159
1.5826−003	1.5665−003	1.5257−003	1.4753−003	1.4284−003	160
1.5570−003	1.5421−003	1.5021−003	1.4530−003	1.4089−003	161
1.5320−003	1.5181−003	1.4789−003	1.4312−003	1.3903−003	162
1.5075−003	1.4945−003	1.4562−003	1.4098−003	1.3660−003	163
1.4836−003	1.4713−003	1.4338−003	1.3888−003	1.3467−003	164
1.4602−003	1.4485−003	1.4118−003	1.3682−003	1.3301−003	165
1.4373−003	1.4260−003	1.3903−003	1.3479−003	1.3072−003	166
1.4149−003	1.4039−003	1.3691−003	1.3280−003	1.2877−003	167
1.3930−003	1.3822−003	1.3482−003	1.3084−003	1.2722−003	168
1.3716−003	1.3608−003	1.3278−003	1.2892−003	1.2506−003	169
1.3506−003	1.3398−003	1.3078−003	1.2703−003	1.2307−003	170
1.3301−003	1.3192−003	1.2881−003	1.2518−003	1.2162−003	171
1.3100−003	1.2990−003	1.2688−003	1.2336−003	1.1963−003	172
1.2904−003	1.2791−003	1.2499−003	1.2158−003	1.1766−003	173
1.2711−003	1.2597−003	1.2314−003	1.1983−003	1.1633−003	174
1.2523−003	1.2406−003	1.2132−003	1.1812−003	1.1459−003	175
1.2339−003	1.2219−003	1.1953−003	1.1643−003	1.1266−003	176
1.2158−003	1.2036−003	1.1778−003	1.1478−003	1.1141−003	177
1.1981−003	1.1857−003	1.1607−003	1.1315−003	1.0987−003	178
1.1808−003	1.1681−003	1.1438−003	1.1155−003	1.0798−003	179
1.1638−003	1.1510−003	1.1273−003	1.0997−003	1.0677−003	180
1.1471−003	1.1342−003	1.1111−003	1.0843−003	1.0546−003	181
1.1308−003	1.1178−003	1.0952−003	1.0691−003	1.0367−003	182
1.1148−003	1.1017−003	1.0796−003	1.0542−003	1.0250−003	183
1.0992−003	1.0860−003	1.0643−003	1.0396−003	1.0137−003	184
1.0838−003	1.0707−003	1.0494−003	1.0253−003	9.9633−004	185
1.0687−003	1.0558−003	1.0347−003	1.0114−003	9.8381−004	186
1.0540−003	1.0411−003	1.0202−003	9.9779−004	9.7351−004	187
1.0395−003	1.0268−003	1.0061−003	9.8441−004	9.5693−004	188
1.0253−003	1.0128−003	9.9230−004	9.7131−004	9.4391−004	189
1.0113−003	9.9909−004	9.7875−004	9.5849−004	9.3483−004	190

LOW FREQUENCY COMPONENT OF THE ELECTRIC MICROFIELDS

$r_0/D=0$	$=0.2$	$=0.4$	$=0.6$	$=0.8$	10β
9.9766−004	9.8567−004	9.6548−004	9.4582−004	9.1956−004	191
9.8425−004	9.7253−004	9.5249−004	9.3337−004	9.0622−004	192
9.7109−004	9.5966−004	9.3977−004	9.2114−004	8.9832−004	193
9.5817−004	9.4703−004	9.2732−004	9.0905−004	8.8498−004	194
9.4550−004	9.3465−004	9.1513−004	8.9714−004	8.7181−004	195
9.3306−004	9.2251−004	9.0321−004	8.8547−004	8.6485−004	196
9.2085−004	9.1060−004	8.9154−004	8.7397−004	8.5314−004	197
9.0887−004	8.9892−004	8.8012−004	8.6268−004	8.3942−004	198
8.9710−004	8.8745−004	8.6895−004	8.5167−004	8.3222−004	199
8.8554−004	8.7620−004	8.5801−004	8.4087−004	8.2177−004	200
8.7420−004	8.6516−004	8.4729−004	8.3025−004	8.0788−004	201
8.6305−004	8.5433−004	8.3680−004	8.1991−004	8.0060−004	202
8.5211−004	8.4370−004	8.2653−004	8.0975−004	7.9175−004	203
8.4136−004	8.3328−004	8.1645−004	7.9974−004	7.7797−004	204
8.3080−004	8.2306−004	8.0657−004	7.8996−004	7.7011−004	205
8.2042−004	8.1304−004	7.9688−004	7.8035−004	7.6243−004	206
8.1023−004	8.0321−004	7.8738−004	7.7086−004	7.4890−004	207
8.0021−004	7.9359−004	7.7805−004	7.6159−004	7.4041−004	208
7.9037−004	7.8417−004	7.6890−004	7.5251−004	7.3411−004	209
7.8069−004	7.7495−004	7.5993−004	7.4357−004	7.2164−004	210
7.7118−004	7.6593−004	7.5114−004	7.3485−004	7.1292−004	211
7.6184−004	7.5711−004	7.4254−004	7.2636−004	7.0807−004	212
7.5265−004	7.4850−004	7.3413−004	7.1801−004	6.9702−004	213
7.4361−004	7.4008−004	7.2591−004	7.0988−004	6.8795−004	214
7.3473−004	7.3186−004	7.1787−004	7.0196−004	6.8401−004	215
7.2600−004	7.2384−004	7.1001−004	6.9417−004	6.7430−004	216
7.1741−004	7.1600−004	7.0233−004	6.8654−004	6.6469−004	217
7.0896−004	7.0834−004	6.9480−004	6.7910−004	6.6118−004	218
7.0066−004	7.0084−004	6.8741−004	6.7174−004	6.5294−004	219
6.9249−004	6.9351−004	6.8016−004	6.6447−004	6.4302−004	220
6.8445−004	6.8631−004	6.7301−004	6.5735−004	6.3973−004	221
6.7654−004	6.7925−004	6.6596−004	6.5028−004	6.3308−004	222
6.6876−004	6.7229−004	6.5898−004	6.4325−004	6.2301−004	223
6.6111−004	6.6543−004	6.5206−004	6.3632−004	6.1949−004	224
6.5358−004	6.5864−004	6.4518−004	6.2941−004	6.1419−004	225
6.4617−004	6.5191−004	6.3833−004	6.2248−004	6.0400−004	226
6.3887−004	6.4523−004	6.3149−004	6.1562−004	5.9978−004	227
6.3169−004	6.3858−004	6.2465−004	6.0876−004	5.9553−004	228
6.2463−004	6.3194−004	6.1781−004	6.0186−004	5.8535−004	229
6.1767−004	6.2530−004	6.1095−004	5.9498−004	5.8011−004	230
6.1082−004	6.1867−004	6.0409−004	5.8812−004	5.7664−004	231
6.0408−004	6.1202−004	5.9721−004	5.8121−004	5.6671−004	232
5.9745−004	6.0536−004	5.9033−004	5.7434−004	5.6033−004	233
5.9091−004	5.9870−004	5.8346−004	5.6752−004	5.5742−004	234
5.8448−004	5.9203−004	5.7661−004	5.6069−004	5.4806−004	235
5.7814−004	5.8536−004	5.6981−004	5.5395−004	5.4062−004	236
5.7190−004	5.7871−004	5.6306−004	5.4733−004	5.3810−004	237
5.6575−004	5.7209−004	5.5640−004	5.4080−004	5.2970−004	238
5.5970−004	5.6551−004	5.4985−004	5.3441−004	5.2149−004	239
5.5373−004	5.5898−004	5.4343−004	5.2825−004	5.1931−004	240
5.4786−004	5.5253−004	5.3716−004	5.2226−004	5.1230−004	241
5.4207−004	5.4617−004	5.3107−004	5.1649−004	5.0377−004	242
5.3637−004	5.3991−004	5.2517−004	5.1103−004	5.0189−004	243
5.3075−004	5.3377−004	5.1948−004	5.0580−004	4.9664−004	244
5.2522−004	5.2775−004	5.1400−004	5.0082−004	4.8824−004	245

LOW FREQUENCY COMPONENT OF THE ELECTRIC MICROFIELDS

$r_0/D=0$	$=0.2$	$=0.4$	$=0.6$	$=0.8$	10β
5.1976−004	5.2185−004	5.0873−004	4.9617−004	4.8657−004	246
5.1438−004	5.1609−004	5.0366−004	4.9176−004	4.8319−004	247
5.0909−004	5.1046−004	4.9878−004	4.8754−004	4.7522−004	248
5.0387−004	5.0495−004	4.9408−004	4.8358−004	4.7346−004	249
4.9872−004	4.9956−004	4.8952−004	4.7979−004	4.7171−004	250
4.9364−004	4.9364−004	4.9364−004	4.7607−004	4.6423−004	251
4.8864−004	4.8864−004	4.8864−004	4.7247−004	4.6187−004	252
4.8371−004	4.8371−004	4.8371−004	4.6890−004	4.6119−004	253
4.7885−004	4.7885−004	4.7885−004	4.6527−004	4.5408−004	254
4.7406−004	4.7406−004	4.7406−004	4.6160−004	4.5058−004	255
4.6934−004	4.6934−004	4.6934−004	4.5786−004	4.5034−004	256
4.6468−004	4.6468−004	4.6468−004	4.5395−004	4.4350−004	257
4.6008−004	4.6008−004	4.6008−004	4.4992−004	4.3857−004	258
4.5555−004	4.5555−004	4.5555−004	4.4579−004	4.3829−004	259
4.5108−004	4.5108−004	4.5108−004	4.4148−004	4.3188−004	260
4.4667−004	4.4667−004	4.4667−004	4.3704−004	4.2559−004	261
4.4233−004	4.4233−004	4.4233−004	4.3254−004	4.2505−004	262
4.3804−004	4.3804−004	4.3804−004	4.2793−004	4.1938−004	263
4.3381−004	4.3381−004	4.3381−004	4.2324−004	4.1209−004	264
4.2964−004	4.2964−004	4.2964−004	4.1858−004	4.1122−004	265
4.2552−004	4.2552−004	4.2552−004	4.1390−004	4.0666−004	266
4.2146−004	4.2146−004	4.2146−004	4.0923−004	3.9887−004	267
4.1745−004	4.1745−004	4.1745−004	4.0467−004	3.9766−004	268
4.1350−004	4.1350−004	4.1350−004	4.0019−004	3.9446−004	269
4.0960−004	4.0960−004	4.0960−004	3.9577−004	3.8665−004	270
4.0575−004	4.0575−004	4.0575−004	3.9153−004	3.8501−004	271
4.0195−004	4.0195−004	4.0195−004	3.8743−004	3.8323−004	272
3.9820−004	3.9820−004	3.9820−004	3.8342−004	3.7578−004	273
3.9450−004	3.9450−004	3.9450−004	3.7960−004	3.7359−004	274
3.9084−004	3.9084−004	3.9084−004	3.7594−004	3.7307−004	275
3.8724−004	3.8724−004	3.8724−004	3.7238−004	3.6628−004	276
3.8368−004	3.8368−004	3.8368−004	3.6898−004	3.6339−004	277
3.8017−004	3.8017−004	3.8017−004	3.6573−004	3.6384−004	278
3.7670−004	3.7670−004	3.7670−004	3.6255−004	3.5789−004	279
3.7327−004	3.7327−004	3.7327−004	3.5950−004	3.5415−004	280
3.6989−004	3.6989−004	3.6989−004	3.5657−004	3.5515−004	281
3.6656−004	3.6656−004	3.6656−004	3.5369−004	3.5009−004	282
3.6326−004	3.6326−004	3.6326−004	3.5087−004	3.4539−004	283
3.6001−004	3.6001−004	3.6001−004	3.4817−004	3.4644−004	284
3.5679−004	3.5679−004	3.5679−004	3.4547−004	3.4231−004	285
3.5362−004	3.5362−004	3.5362−004	3.4279−004	3.3669−004	286
3.5049−004	3.5049−004	3.5049−004	3.4019−004	3.3746−004	287
3.4739−004	3.4739−004	3.4739−004	3.3757−004	3.3441−004	288
3.4434−004	3.4434−004	3.4434−004	3.3493−004	3.2818−004	289
3.4132−004	3.4132−004	3.4132−004	3.3234−004	3.2845−004	290
3.3834−004	3.3834−004	3.3834−004	3.2972−004	3.2648−004	291
3.3539−004	3.3539−004	3.3539−004	3.2704−004	3.1980−004	292
3.3248−004	3.3248−004	3.3248−004	3.2442−004	3.1914−004	293
3.2961−004	3.2961−004	3.2961−004	3.2178−004	3.1799−004	294
3.2677−004	3.2677−004	3.2677−004	3.1910−004	3.1103−004	295
3.2396−004	3.2396−004	3.2396−004	3.1647−004	3.0924−004	296
3.2119−004	3.2119−004	3.2119−004	3.1387−004	3.0888−004	297
3.1845−004	3.1845−004	3.1845−004	3.1124−004	3.0222−004	298
3.1575−004	3.1575−004	3.1575−004	3.0867−004	2.9956−004	299
3.1307−004	3.1307−004	3.1307−004	3.0614−004	3.0015−004	300

U. S. GOVERNMENT PRINTING OFFICE : 1971 O - 406-848

Latest developments in the subject area of this publication, as well as in other areas where the National Bureau of Standards is active, are reported in the NBS Technical News Bulletin. See following page.

HOW TO KEEP ABREAST OF NBS ACTIVITIES

Your purchase of this publication indicates an interest in the research, development, technology, or service activities of the National Bureau of Standards.

The best source of current awareness in your specific area, as well as in other NBS programs of possible interest, is the TECHNICAL NEWS BULLETIN, a monthly magazine designed for engineers, chemists, physicists, research and product development managers, librarians, and company executives.

If you do not now receive the TECHNICAL NEWS BULLETIN and would like to subscribe, and/or to review some recent issues, please fill out and return the form below.

Mail to: Office of Technical Information and Publications
National Bureau of Standards
Washington, D. C. 20234

Name _____

Affiliation _____

Address _____

City _____ State _____ Zip _____

☐ Please send complimentary past issues of the Technical News Bulletin.

☐ Please enter my 1-yr subscription. Enclosed is my check or money order for $3.00 (additional $1.00 for foreign mailing).
Check is made payable to: SUPERINTENDENT OF DOCUMENTS.

Monogr. 120

(cut here)

NBS TECHNICAL PUBLICATIONS

PERIODICALS

JOURNAL OF RESEARCH reports National Bureau of Standards research and development in physics, mathematics, chemistry, and engineering. Comprehensive scientific papers give complete details of the work, including laboratory data, experimental procedures, and theoretical and mathematical analyses. Illustrated with photographs, drawings, and charts.

Published in three sections, available separately:

• Physics and Chemistry

Papers of interest primarily to scientists working in these fields. This section covers a broad range of physical and chemical research, with major emphasis on standards of physical measurement, fundamental constants, and properties of matter. Issued six times a year. Annual subscription: Domestic, $9.50; foreign, $11.75*.

• Mathematical Sciences

Studies and compilations designed mainly for the mathematician and theoretical physicist. Topics in mathematical statistics, theory of experiment design, numerical analysis, theoretical physics and chemistry, logical design and programming of computers and computer systems. Short numerical tables. Issued quarterly. Annual subscription: Domestic, $5.00; foreign, $6.25*.

• Engineering and Instrumentation

Reporting results of interest chiefly to the engineer and the applied scientist. This section includes many of the new developments in instrumentation resulting from the Bureau's work in physical measurement, data processing, and development of test methods. It will also cover some of the work in acoustics, applied mechanics, building research, and cryogenic engineering. Issued quarterly. Annual subscription: Domestic, $5.00; foreign, $6.25*.

TECHNICAL NEWS BULLETIN

The best single source of information concerning the Bureau's research, developmental, cooperative and publication activities, this monthly publication is designed for the industry-oriented individual whose daily work involves intimate contact with science and technology—*for engineers, chemists, physicists, research managers, product-development managers, and company executives.* Annual subscription: Domestic, $3.00; foreign, $4.00*.

* Difference in price is due to extra cost of foreign mailing.

NONPERIODICALS

Applied Mathematics Series. Mathematical tables, manuals, and studies.

Building Science Series. Research results, test methods, and performance criteria of building materials, components, systems, and structures.

Handbooks. Recommended codes of engineering and industrial practice (including safety codes) developed in cooperation with interested industries, professional organizations, and regulatory bodies.

Special Publications. Proceedings of NBS conferences, bibliographies, annual reports, wall charts, pamphlets, etc.

Monographs. Major contributions to the technical literature on various subjects related to the Bureau's scientific and technical activities.

National Standard Reference Data Series. NSRDS provides quantitative data on the physical and chemical properties of materials, compiled from the world's literature and critically evaluated.

Product Standards. Provide requirements for sizes, types, quality and methods for testing various industrial products. These standards are developed cooperatively with interested Government and industry groups and provide the basis for common understanding of product characteristics for both buyers and sellers. Their use is voluntary.

Technical Notes. This series consists of communications and reports (covering both other agency and NBS-sponsored work) of limited or transitory interest.

Federal Information Processing Standards Publications. This series is the official publication within the Federal Government for information on standards adopted and promulgated under the Public Law 89–306, and Bureau of the Budget Circular A–86 entitled, Standardization of Data Elements and Codes in Data Systems.

Order NBS publications from:

Superintendent of Documents
Government Printing Office
Washington, D.C. 20402

U.S. DEPARTMENT OF COMMERCE
WASHINGTON, D.C. 20230

OFFICIAL BUSINESS

PENALTY FOR PRIVATE USE, $300

POSTAGE AND FEES PAID
U.S. DEPARTMENT OF COMMERCE